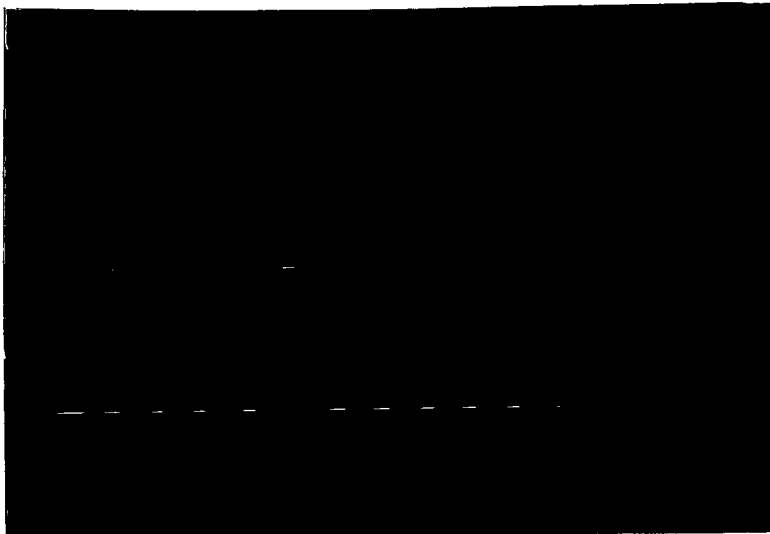


2  
mix

NRC-72-14



(NASA-CR-124177) DESIGN, FABRICATION,  
ASSEMBLY AND DELIVERY OF A LABORATORY  
PROTOTYPE OF A RESIDUAL GAS ANALYZER  
Final Report (National Research Corp.)  
75 p HC \$5.75

N73-21386

Unclas

CSSL 14B G3/14 17512

**NRC** : : : NATIONAL RESEARCH CORPORATION  
: : : A SUBSIDIARY OF CABOT CORPORATION  
: : : BILLERICA, MASSACHUSETTS 01821

15

FINAL REPORT

DESIGN, FABRICATION, ASSEMBLY AND  
DELIVERY OF A LABORATORY PROTOTYPE  
OF A RESIDUAL GAS ANALYZER

By

W. S. Kreisman  
F. L. Torney  
J. R. Roehrig

November 22, 1972

Prepared Under Contract No. NAS8-27877

By

National Research Corporation  
(A Subsidiary of Cabot Corporation)  
70 Memorial Drive  
Cambridge, Massachusetts 02142

For

NATIONAL AERONAUTICS AND SPACE ADMINISTRATION

i

PRECEDING PAGE BLANK NOT FILMED

TABLE OF CONTENTS

|  | <u>Page No.</u> |
|--|-----------------|
| SUMMARY.....   | 1               |
| INTRODUCTION.....                                    | 2               |
| LIST OF SYMBOLS AND ABBREVIATIONS.....               | 4               |
| SYSTEM DESIGN GOALS AND GUIDELINES.....              | 7               |
| THEORETICAL BASIS OF QUADRUPOLE ANALYZER DESIGN..... | 8               |
| DESIGN APPROACH.....                                 | 13              |
| General Considerations.....                          | 13              |
| Specific Quadrupole Design.....                      | 21              |
| Ion Source Design.....                               | 26              |
| Multiplier Design.....                               | 27              |
| Electronic System Design.....                        | 29              |
| Rf Generator.....                                    | 29              |
| Sweep Circuits.....                                  | 30              |
| Electrometer.....                                    | 30              |
| Power Supply.....                                    | 31              |
| SYSTEM CONSTRUCTION.....                             | 32              |
| DEVELOPMENT AND TEST RESULTS.....                    | 40              |
| Ion Source.....                                      | 40              |
| Quadrupole Analyzer.....                             | 51              |
| Electron Multiplier.....                             | 53              |
| Electronic Development.....                          | 55              |

|  |    |
|--|----|
| Rf Generator.....                            | 55 |
| Electrometer.....                            | 56 |
| OPERATIONAL CHARACTERISTICS.....             | 57 |
| General.....                                 | 57 |
| Operational Characteristics.....             | 58 |
| Discussion of Performance.....               | 59 |
| Resolution.....                              | 59 |
| Sensitivity.....                             | 61 |
| Dynamic Range and Signal to Noise Ratio..... | 67 |
| Linearity.....                               | 68 |
| Mass Range.....                              | 68 |
| Special Features.....                        | 68 |
| Bake-Out Heaters.....                        | 68 |
| Ion Source Entrance Ports.....               | 69 |
| Multiplier Gain Measurements.....            | 69 |
| Total Cathode Current (Ion Source).....      | 70 |
| CONCLUSIONS.....                             | 70 |

## LIST OF FIGURES

| Figure No. | Title   | Page No. |
|------------|---|----------|
| 1          | SCHEMATIC BLOCK DIAGRAM OF PROTOTYPE RGA  | 14       |
| 2          | PROTOTYPE RGA WITH TEMPORARY FLANGES  | 33       |
| 3          | CONSTRUCTION DETAILS OF THE RGA COLD CATHODE ION SOURCE                               | 34       |
| 4          | CONSTRUCTION DETAILS OF THE RGA QUADRUPOLE ANALYZER                                   | 37       |
| 5          | CONSTRUCTION DETAILS OF RGA DETECTOR  | 39       |
| 6          | PHOTOGRAPH OF LABORATORY PROTOTYPE RGA  | 41       |
| 7          | PROTOTYPE RGA ION SOURCE TEST FLANGE ASSEMBLY   | 43       |
| 8          | PROTOTYPE RGA ION SOURCE VACUUM TEST SYSTEM WITH INSTALLED ION SOURCE AND TEST FLANGE | 44       |
| 9          | MAGNETIC FIELD STRENGTHS WITHIN AND OUTSIDE THE ION SOURCE CYLINDRICAL MAGNET         | 45       |
| 10         | EQUIPMENT AND ELECTRICAL CONNECTIONS USED TO MEASURE ION ENERGIES                     | 47       |
| 11         | PROTOTYPE RGA ION SOURCE ENERGY DISTRIBUTION  | 49       |
| 12         | PROTOTYPE ION SOURCE SENSITIVITY CURVES FOR NITROGEN GAS                              | 50       |
| 13         | SPECTRUM OF INERT GASES AND TUNGSTEN HEXAFLUORIDE AND SYSTEM RESIDUALS                | 60       |
| 14         | SPECTRUM OF ARGON AND RESIDUALS   | 64       |

DESIGN, FABRICATION, ASSEMBLY, AND DELIVERY  
OF A LABORATORY PROTOTYPE OF A  
RESIDUAL GAS ANALYZER

By

W. S. Kreisman, F. L. Torney, and J. R. Roehrig

National Research Corporation  
(A Subsidiary of Cabot Corporation)

SUMMARY

This report describes the design, development, and test of a wide mass range residual gas analyzer which will be one component of an Integrated Real Time Contamination Monitor System. The instrument has been developed and tested to the laboratory prototype phase, demonstrating the performance that can be expected from a flight instrument of similar design.

The instrument's analyzer is of the quadrupole type and a cold cathode ion source is employed as the ionizer. The associated electronics supply all necessary operating and mass sweep voltages for the ionizer, analyzer and electron multiplier ion detector. The instrument features a very fast linear electrometer with automatic range changing. The full mass range of 2 to 300 amu is automatically and repetitively scanned every sixty seconds and suitable telemetry outputs are provided for intensity and mass identification as well as a digital identification of the electrometer range. The instrument has an ultimate partial pressure sensitivity for nitrogen of approximately  $1 \times 10^{-9}$  Torr with a dynamic range of detectability of better than  $10^4:1$ . The nominal operating range of total pressures is from  $10^{-4}$  Torr to approximately  $5 \times 10^{-8}$  Torr.

|

Other special features are also provided, such as bake-out heaters for the ion source and analyzer (including temperature monitors). The ion source is also equipped with two transverse entrance ports oriented 180° apart so that gaseous fluxes may be detected from opposite directions if desired. The complete package requires an average power of approximately 38 watts (not including bakeout heaters) from a 28 volt source. The package weighs less than 16.5 lbs.

#### INTRODUCTION

It is well known that outgassing of various spacecraft materials, even at very low levels, can create a dangerous breathing environment in closed manned space cabins and can also coat critical optical and thermal control surfaces with performance degrading layers. To minimize such contamination, it is necessary to identify and eliminate or reduce the sources of the contaminants. Excessive outgassing of spacecraft materials, such as electrical insulation for example, also accompanies the deterioration of these materials. Measurements of outgassing products can serve to detect the presence of these degradation processes and thus help avoid component failure.

The purpose of the development program described in this report was to design, fabricate, and deliver a laboratory prototype of a Residual Gas Analyzer (RGA) which would be used in conjunction with other instruments to monitor and identify

contamination in the vicinity of sensitive spacecraft instruments. The complete monitoring system was designated as a Real Time Contamination Monitor. The RGA portion of the system was to serve as a mass spectrometer analyzer having a wide mass range, moderate resolving power, and a wide dynamic range.

The identification of gaseous contaminants such as hydrocarbons, plasticizers, and various solvents used in connection with paints and coatings can be accomplished with a mass spectrometer. A wide mass range of several hundred atomic mass units would be required to detect the large organic molecules that are characteristic of spacecraft component outgassing. Sufficient resolving power would be required to separate adjacent masses at the high mass end of the mass scale. It was anticipated that computer techniques would be used to completely separate masses that were only partially separated by the RGA. A wide dynamic range would be required to simultaneously detect both major concentrations and trace concentrations of contaminant gases.

An RGA that is designed to be operated aboard a space vehicle must be compact, light in weight, low in power consumption and built to withstand shock, vibration and thermal vacuum environmental conditions. Flight-type mass spectrometers of various kinds conforming to the above requirements have been constructed, but, generally, their mass ranges have been limited to approximately 40 or 50 atomic mass units. Ordinarily, the measurement of higher masses requires larger instruments that consume large amounts of power.



It was decided to use an rf quadrupole mass spectrometer analyzer, in combination with a cold cathode ion source and an off-axis electron multiplier for the RGA. All solid state electronics were used to power and control the ion source, analyzer, and electron multiplier. The cold cathode ion source kept the power requirements low, minimized self contamination and provided high reliability (no filament to burn out). The quadrupole analyzer furnished the required wide mass range and resolution with a minimum volume and weight, while the off-axis electron multiplier provided the needed gain and wide dynamic range.

#### LIST OF SYMBOLS AND ABBREVIATIONS

|          |   |
|----------|---|
| a        | U/V ratio (see below)   |
| BA Gauge | Bayard-Alpert Gauge. Also BAG   |
| b        | A constant sweep off-set voltage (volts).<br>See eqs. (10 and 11)           |
| C        | Total capacitance of quadrupole and output tank<br>circuit (pF)             |
| D        | Deflection distance of ion beam off axis at<br>multiplier                   |
| $D_{in}$ | Maximum quadrupole entrance aperture diameter for<br>100% transmission (cm) |

|              |   |
|--------------|---|
| $d$          | Spacing between electron multiplier deflection plates.                        |
| $E_t$        | Maximum transverse ion energy for 100% transmission (volts)                   |
| $L$          | Length of quadrupole rods (cm)  |
| $L'$         | Distance from center of deflecting plates to multiplier first dynode          |
| $l$          | Length of deflecting plates   |
| $M$          | Ionic mass (amu)  |
| $M_{MAX}$    | Maximum value of $M$ to be measured (amu)                                     |
| $\Delta M$   | Peak width at base of peak (amu)  |
| $M/\Delta M$ | Resolving power   |
| $P$          | Power required to operate quadrupole, referred to output tank circuit (watts) |
| $P_t$        | Peak power required by tank circuit at $M_{MAX}$ (watts)                      |
| $Q$          | Figure of merit of the output tank circuit                                    |
| $R_{rod}$    | Radius of quadrupole rods (cm)  |
| $r_o$        | Radius of circle inscribed between the quadrupole rods (cm)                   |
| $\Delta r_o$ | Incremental change in $r_o$ (cm)  |

|               |   |
|---------------|---|
| RGA           | Residual Gas Analyzer   |
| U             | Dc voltage applied to the quadrupole rods (volts)                   |
| $\Delta U$    | Incremental change in U (volts)                                     |
| $U_a$         | Maximum axial ion energy (volts)                                    |
| U/V           | Ratio of dc/rf voltage applied to rods. Also referred to as "a"     |
| V             | Peak rf voltage applied to quadrupole rods with U (volts)           |
| $\Delta V$    | Incremental change in V (volts)                                     |
| $V_{MAX}$     | Value of V at $M_{MAX}$   |
| $V_{in}$      | Actual ion energy entering quadrupole (volts)                       |
| $V_{in(MAX)}$ | Maximum axial ion energy (volts)                                    |
| $V_a$         | Axial energy of ions entering multiplier after acceleration (volts) |
| $V_d$         | Potential between multiplier deflector plates. (volts)              |
| $\theta$      | Ion beam half angle entering quadrupole (degrees)                   |
| $\theta_s$    | Ion beam half angle leaving ion source (degrees)                    |
| $\nu$         | rf drive frequency (mHz)  |
| $\Delta \nu$  | Incremental change in $\nu$ (mHz)                                   |

## SYSTEM DESIGN GOALS AND GUIDELINES

The objective of this program was to design, fabricate and deliver a laboratory prototype of a Residual Gas Analyzer (RGA). Past experience was to be used as the state-of-the-art to develop techniques to achieve the design goals and guideline specifications listed below. It was desired that the design be practical with emphasis on long term accuracy and stability, cleanability, low cost, and good producibility with detailed quality requirements. Specific design goals are listed below:

1. Mass Range of 0-300 amu.
2. Output data read by either an 8 or 10 bit A to D converter (not furnished).
3. Total power consumption not to exceed 25 watts.
4. A cold cathode magnetron discharge type ion source.
5. An upper size limit of 6" x 6" x 20".
6. Two output data channels of 0 to plus 5 volts.
7. Not over three input command channels.
8. A dynamic range between  $10^4$  and  $10^6$ .
9. Capability of operating in a water vapor environment of  $10^{-4}$  Torr for at least 24 hours.
10. Provision for telemetry voltages proportional to critical operating parameters such as the source anode voltage, electron multiplier voltage, etc.
11. Construction in accordance with MSFC contamination criteria as specified in "Apollo Telescope Mount Materials Control for Contamination Due to Outgassing", ATM Document Number 50MO2442, Revision U dated March 1, 1971.

## THEORETICAL BASIS OF QUADRUPOLE ANALYZER DESIGN

As stated in the introduction, the residual gas analyzer consisted of three major components; a cold cathode ion source an rf quadrupole mass spectrometer analyzer, and an off-axis electron multiplier ion detector, together with their associated electronics.

It was recognized early in the project that the basic problem was to modify an existing rf quadrupole type mass spectrometer of flight design so that it would cover a much wider mass range than it normally does and still maintain acceptable parameters of size, weight, power, sensitivity, resolution and dynamic range.

The most significant of the problems to be solved in this modification concerned the quadrupole analyzer itself. Therefore, a brief discussion of quadrupole theory will be given to outline the major areas of design concentration and provide the reader with a better understanding of the instrument.

In Prof. Pauls' original paper, published in 1953, the field forming surfaces of the quadrupole electric mass filter were chosen to be hyperbolic in cross-section. These surfaces are theoretically optimum for the mass selection of ions transmitted by the filter. Subsequently, it was discovered that circular cross-section rods could be substituted for the hyperbolic section rods with no major degradation of the quadrupole field. The power required to operate a quadrupole analyzer with either round or hyperbolic rods is given by:

$$P = \frac{6.5 \times 10^{-4} C M^2 v^5 r_o^4}{Q} \text{ watts} \quad (1)$$

where C is the total capacitance in the rf output tank circuit in pf, M is the ionic mass in amu,  $\nu$  is the rf drive frequency in MHz,  $r_0$  is the radius of the circle inscribed between the quadrupole rods in cm, and Q is the figure of merit of the output tank circuit driving the rods. From this equation, it can be seen that M,  $\nu$  and  $r_0$  are the most important parameters affecting power. Similarly, M,  $\nu$  and  $r_0$  are also important factors affecting the resolving power of the spectrometer, as is shown by the following equations:

$$\text{Resolving Power} = \frac{M}{\Delta M} \approx \frac{0.126}{0.16784 - U/V} \quad (2)$$

where U is the dc voltage applied to the rods and V is the peak rf voltage applied simultaneously with U\*.  $\Delta M$  is the peak width (in amu) at the base of the peak. If the U/V ratio is held constant (also  $\nu$ ), the resolving power will be constant. This is one mode of operating the instrument, although not the preferred one for the present application.

Now, the rf voltage V, is a function of M,  $\nu$  and  $r_0$  as is shown by the next equation:

$$V = 7.219 M \nu^2 r_0^2 \text{ volts} \quad (3)$$

where the parameters are as defined in equation (1). Thus we see that power and resolution are interrelated through the parameters M,  $\nu$  and  $r_0$ .

---

\* The rod voltages are  $\pm \phi$  where  $\phi = U + V \cos 2\pi \nu t$ .

The extension of a quadrupole's mass range (and resolving power) requires additional attention to dimensional tolerances and the assembly accuracy of the analyzer. Both theory and practice show that the required dimensional tolerance,  $\Delta r_0$ , for  $r_0$  is related to the resolving power by:

$$\frac{\Delta r_0}{r_0} = 1/4 \left( \frac{\Delta M}{M} \right) \quad (4)$$

In a similar fashion, the frequency and voltage tolerances are:

$$\frac{\Delta \nu}{\nu} = 1/4 \left( \frac{\Delta M}{M} \right) \quad (5)$$

$$\frac{\Delta U}{U} = \frac{\Delta V}{V} = 1/2 \left( \frac{\Delta M}{M} \right) \quad (6)$$

Obviously, the largest possible value of  $r_0$  should be chosen to ease the dimensional tolerances of construction and assembly. However, as equation (1) shows, the required power increases as  $r_0^4$ . Briefly then, to extend the mass range,  $r_0$  must be carefully chosen to keep power requirements within bounds. The next section discusses these requirements in detail.

Having selected values for  $r_0$ ,  $\nu$  and  $V$ , one of the last remaining quadrupole design parameter to be chosen is the length of the rods. It has been found experimentally that ions must remain in the quadrupole field  $5\sqrt{M/\Delta M}$  cycles to insure mass

selection. An upper limit exists therefore on the axial component of ion velocity or energy. This limit is given by the following equation:

$$U_a \approx 2.1 \times 10^{-2} v^2 L^2 \Delta M \text{ volts} \quad (7)$$

where  $U_a$  is the maximum axial ion energy expressed in volts and  $L$  is the rod length in cm. The other parameters are dimensioned according to equation (1).

For ions injected parallel to the quadrupole axis, the maximum injection aperture to insure that none of the ions will strike the electrodes has a diameter  $D_{in}$  given by the equation below:

$$D_{in} \approx 0.8 r_o \sqrt{\frac{\Delta M}{M}} \quad (8)$$

Similarly, the maximum transverse energy  $E_t$  that an ion injected on the axis can have if its transmission is to be insured is given by the expression:

$$E_t \approx \frac{V \Delta M}{30 M} \quad (9)$$

The nature of the relationship between the dc voltage  $U$  and the rf voltage  $V$  determines the mode in which the quadrupole will be operated. It is common practice today to provide a dc voltage  $U$  which is linearly related to  $V$  as follows:



$$U = aV - b \quad (10)$$

where a and b are fixed constants.

If the constant "offset" voltage b is made equal to zero, the quadrupole U/V ratio is constant and equation (2) indicates that the instrument will have a constant resolution.

In terms of equation (10), one can derive the following expression for the peak width  $\Delta M$ :

$$\Delta M \cong 7.94 (0.16784 - a) M + \frac{1.10 b}{v^2 r_o^2} \text{ amu} \quad (11)$$

As can be seen, if the constant a is made equal to 0.16784, the value of  $\Delta M$  will be a constant independent of the mass M. This mode of operation is called the constant peak width mode.

## DESIGN APPROACH

### General Considerations

The overall design of the prototype RGA is illustrated schematically in Figure 1. The system consisted of mechanical and electronic components interconnected as shown. The gas to be analyzed entered the cold cathode ion source from either of two tubulations 180 degrees apart, and a fraction of the molecules were ionized in the high voltage magnetically confined discharge of the source. A fraction of the ions from the source entered the rf quadrupole analyzer where a combination of rf and dc electric fields allowed only ions of a specific mass-to-charge ratio to be transmitted to the ion detector. By varying the rf and dc electric fields via the rf/dc generator and control amplifier, ions having successively larger mass-to-charge ratios would be transmitted by the analyzer and detected. An analog signal proportional to the ion mass peak height was provided by a linear, automatic range switching electrometer. An analog signal proportional to the ion mass was obtained from the rf/dc generator. Test points provided voltages that were a measure of the dc rod voltage, the rf frequency, the ion current to the electron multiplier first dynode (to provide a measure of the relative multiplier gain), the ion source total cathode current ( a measure of the ion source pressure), and the temperatures of the ion source and ion detector. A positive output high voltage power supply provided an adjustable voltage for the anode of the cold cathode ion source. A negative output high voltage power supply provided an adjustable voltage for the electron multiplier. A dc/dc converter transformed +28 volt input power to the proper voltages required by the electronics.

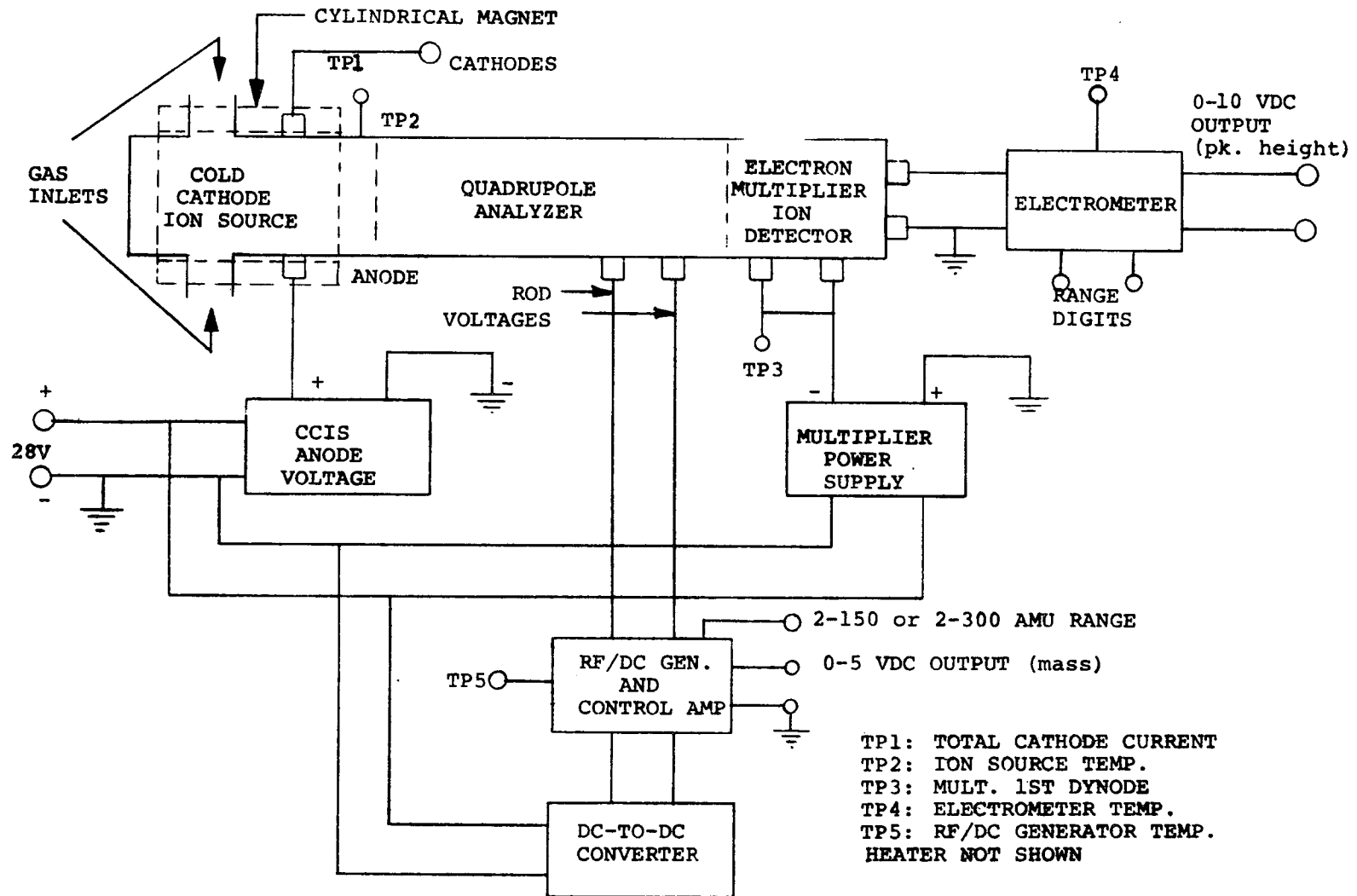


FIGURE 1. - SCHEMATIC BLOCK DIAGRAM OF PROTOTYPE RGA

It was decided early in the program that a cold cathode ion source was preferable to a hot filament ion source for this RGA. The cold cathode source was simpler, cleaner (less outgassing and chemical interaction), more reliable, and had a longer lifetime.

The electron multiplier selected for the RGA was an Allen type 14 stage Be-Cu dynode unit of small size, light weight and high gain capability. This multiplier had a large aperture first dynode so that it could be used in an effective "off-axis" ion collection mode.

The electrometer that was developed for the prototype RGA was of the linear, automatic range switching variety. Since the RGA was designed to have a dynamic range of at least four decades, the electrometer had four current ranges, going from  $1 \times 10^{-9}$  ampere full scale on the lowest range to  $1 \times 10^{-6}$  ampere full scale on the highest current range. A linear electrometer design was chosen over a logarithmic electrometer design in order to obtain higher accuracy and greater stability.

A major decision was made at the beginning of the program to use a single range rf quadrupole analyzer to scan the desired mass range of 0 to 300 amu. The use of a single range rather than two or more ranges to cover all masses resulted in an instrument that was simpler to build and operate and provided higher reliability. Multiple range instruments can improve performance for low and intermediate mass measurements but they do not improve performance for the higher mass measurements.

In order to facilitate the development of the ion source, quadrupole analyzer and electron multiplier ion detector, it was decided to build these three major components of the RGA

as separate subassemblies. Temporary elastomer O-ring type flanges would be provided at the ends of the subassemblies so that they could be fastened together and operated as a single unit when required. In this way, the source, analyzer and detector could be developed and tested either separately or together. Final assembly of the components was performed by machining off the temporary flanges and welding the components together.

In designing a small, low power quadrupole type mass spectrometer having an extended mass range, one must consider the overall design of the instrument. Although the rf quadrupole electric field analyzer is the key element of the system, the ion source and ion detector also play vital roles. If the source ion energies are too high or their angular spread is too great, then the desired resolution and sensitivity cannot be achieved. On the other hand, if the ion detector is not sensitive enough, then one cannot compensate for the loss in sensitivity incurred when the ion beam from the source is decreased in diameter and angular spread.

As discussed previously, the quadrupole analyzer is expected to provide the major limitation to an increase in the mass range. In particular, the dimensional accuracy of the quadrupole rods, whether they are of circular or hyperbolic cross-section, and the accuracy of their alignment is expected to limit the mass resolution attainable at high masses.

The four individual quadrupole rods and their mounting supports must be machined to tolerances of the order of a few hundred micro inches as will be shown. This is entirely possible, but the design of the rods and supports must be carefully planned so that there will be no unacceptable

tolerance build-up and no serious dimension changes as a result of temperature gradients. The voltage and frequency accuracy limitations can generally be met with the use of well-known regulation circuits.

It was anticipated that the four quadrupole rods would be machined from a 300 series stainless steel. Such materials have the required dimensional stability and low temperature coefficients. In addition, they are non-magnetic and are good vacuum materials. Electrically insulating supports were fashioned from machinable ceramic.

Second in importance to the selection of the shape and dimensional accuracy of the quadrupole rods in extending the mass range is the selection of ion injection axial and transverse energies. Ions must be injected close to the instrument axis and have a limited radial energy if they are to be transmitted through the quadrupole rod structure. The conditions that must be satisfied to obtain high (100 percent) transmission of ions are given by equations (8) and (9) of the preceding section. Equation (9) partly determined the beam half angle  $\theta$ , as shown below:

$$\tan^2\theta \cong \frac{V \Delta M}{30 V_{in} M} = \frac{E_t}{V_{in}} \quad (12)$$

where  $\theta$  is the maximum half-angle of the diverging ion beam that is permitted to enter the quadrupole analyzer and  $V_{in}$  is the actual axial ion energy. The other parameters have already been defined.

In theory, by meeting the stringent entrance conditions of equations (8) and (12), 100 percent transmission can be achieved so that there is no mass discrimination within the analyzer. In practice, it is often found that the very small entrance aperture and beam divergence required by equations (8) and (12) reduce the instrument sensitivity to an unacceptably low level for a given resolution. Since there are other discrimination effects that can occur in the source and the multiplier, the attainment of 100 percent transmission is not essential and is usually abandoned. Therefore, the extended mass range instrument was operated at less than 100 percent transmission.

When operating at less than 100 percent transmission, equation (8) indicates that for a given entrance aperture diameter larger than the limiting value  $D_{in}$ , operation in the constant resolution mode produces no mass discrimination, but operation in the constant peak width mode causes discrimination against the high masses (increased values of  $M$  reduce the value of  $D_{in}$ , the diameter of the aperture within which all ions can be collected). Discrimination varies with the square root of the mass and so it is a "weak" discrimination.

Similarly, when operating at less than 100 percent transmission, equation (12) indicates that for a given entrance ion beam half angle larger than the limiting value  $\theta$ , operating in the constant peak width mode produces no mass discrimination, but operation in the constant resolution mode causes discrimination against the low masses (smaller values of  $M$  reduce the value of the angle  $\theta$  within which all masses can be collected). Discrimination varies with the first power of the mass and so it is a "strong" discrimination.

The mass discrimination caused by either of these modes can be reduced by operating in an "in-between" or hybrid mode in which  $\Delta M$  varies by a small amount over the mass range.

In either the constant peak width mode or hybrid mode, the resolution, defined as  $M/\Delta M$ , will vary over the mass range. The resolution will be highest at the high mass end of the range, where it is needed, and correspondingly lower at the low mass end of the range. The maximum resolution attainable will be limited by either the mechanical or electrical tolerances as expressed in equations (4), (5) and (6), by the axial ion energy as expressed by equation (7), by the dc to rf voltage ratio ( $U/V$ ) expressed by equation (2), or by fringe field effects.

The sensitivity of the overall instrument is affected by the ion source sensitivity, the quadrupole transmission and the detector sensitivity. The ion source sensitivity (output ion current for a given pressure of a specific gas) is determined by the ionization efficiency of the gas, the source anode voltage and magnetic field, the geometry of the collimating apertures, and the presence of extraction and focussing (or defocussing) potentials. The quadrupole transmission will depend on the  $U/V$  ratio, the entrance aperture diameter, the entrance ion beam angular divergence, the axial ion energy, the exit aperture diameter, the effects of fringing fields at the ends of the quadrupole rods, and the mass and peak width as discussed above.

Finally, the detector sensitivity is determined by the exiting ion beam angular divergence, the collection efficiency of the multiplier first dynode and the gain of the multiplier for the particular ions. Multiplier gain varies linearly with the ion energy, increases with increasing angle of incidence



of the ions at the first dynode, increases with molecular complexity, but decreases with increasing mass. It is known that the multiplier gain for a given species remains relatively constant over a period of time providing that the dynodes are not contaminated by condensing species or fatigued by overly large ion currents. However, multiplier gain does change gradually over a long period of time and provision must be made to measure such gain changes.

The peak width  $\Delta M$  effectively determines the resolution of the instrument. When operated at a constant frequency, the operating voltages can be adjusted so that the peak width  $\Delta M$  is approximately constant over the mass range. A peak width of 1.0 amu should theoretically allow adjacent peaks to be separated completely down to the baseline (zero valley). A peak width of 1.32 amu should allow adjacent (triangularly-shaped) peaks to be separated at half peak height (that is, with a 50 percent valley). A peak width of 1.80 amu should allow adjacent peaks to be separated with a 90 percent valley. If computer means will be used to help locate and define peaks, values of  $\Delta M$  up to 1.80 amu can be used.

The ion source design was patterned after the design of a cold cathode magnetron ion source that had been developed for use with a double focussing magnetic sector mass spectrometer. One special feature of this design was the isolation of both cathodes from electrical ground so that the source ion beam could be accelerated or retarded before entering the quadrupole. A second special feature of this ion source was the provision of two collimation apertures at the exit cathode to limit the half angle  $\theta$  of the exiting ion beam. The beam angle selected was based on the ion entrance conditions of the quadrupole.

The electron multiplier selected for this system was the small 14 stage Be-Cu unit manufactured by EAL. This multiplier was modified to accept an off-axis ion beam and block an on-axis photon beam. Deflection plates were attached to the front (first dynode end) of the multiplier to deflect the ion beam. The deflection voltage was obtained internally from the dynode resistors. The connection to the first dynode was brought outside the instrument so that it could be used as a Faraday cage to measure ions leaving the quadrupole (before multiplication). This made it possible to obtain a relative measure of the multiplier gain. The first dynode was connected via an external jumper cable to the remaining dynodes for normal use in amplifying the quadrupole output ion current.

The important design parameters of the ion source and electron multiplier will be discussed after the detailed design of the quadrupole analyzer is presented.

#### Specific Quadrupole Design

The design of the quadrupole was carried out by performing calculations for both an ideal "design goal instrument" and a "worst case instrument" in order to determine operating parameters and their interrelationship. The design is arbitrary in the sense that it can be scaled up or down depending on size, weight and power limitations. The system design goals and guidelines do provide such limitations as will be seen.

The design of the quadrupole was started by using past experience to select a value of  $r_0$  and the associated rod diameter that had a chance of meeting the resolution and power requirements. It was decided to start the design by using standard 0.375 inch diameter rods.

$$R_{\text{rod}} = 1.16 r_o = \frac{0.37500''}{2} = 0.18750 \text{ inches}$$

so that

$$r_o = 0.16164'' = 0.41056 \text{ cm}$$

Calculations were carried out using five significant figures even though final parameter values were often rounded off to three or four significant figures. A maximum r.f. voltage of 1500 volts was assumed.

Dimensional Tolerances:

a) Design Goal Instrument,  $\Delta M = 1.32 \text{ amu}$

$$\Delta r_o = \frac{1}{4} \frac{\Delta M}{M_{\text{MAX}}} r_o = \frac{1}{4} \frac{1.32}{300} (0.16164) = 178 \times 10^{-6}''$$

b) Worst Case Instrument,  $\Delta M = 1.80 \text{ amu}$

$$\Delta r_o = \frac{1.80}{1.32} (178 \times 10^{-6}) = 243 \times 10^{-6}''$$

Operating Frequency:

$$\nu^2 = \frac{V_{\text{MAX}}}{7.219 M_{\text{MAX}} r_o^2} = \frac{1500 \text{ Volts}}{7.219 (300) (0.16856)} = 4.1090 \text{ mHz}^2$$

$$\therefore \nu = 2.0271 \text{ mHz}$$

Tank Circuit Power:

$$\begin{aligned} P_t &= \frac{6.5 \times 10^{-4} C M_{MAX}^2 v^5 r_o^4}{Q} \\ &= \frac{6.5 \times 10^{-4} (40 \text{ pf}) (300)^2 (34.226) (0.028412)}{200} \\ &= 11.377 \text{ watts peak at 300 amu} \end{aligned}$$

At 50% efficiency,  $p = 2P_t = 22.754$  watts peak at 300 amu

Maximum Axial Ion Energy:

Assume a rod length of 8.0000".

a) Design Goal Instrument,  $\Delta M = 1.32$  amu

$$\begin{aligned} V_{in(MAX)} &= 0.021 L^2 v^2 \Delta M \\ &= 0.021 (412.90) (4.1090) (1.32) \\ &= 47.030 \text{ Volts} \end{aligned}$$

b) Worst Case Instrument,  $\Delta M = 1.80$  amu

$$V_{in(MAX)} = \frac{1.80}{1.32} (47.030) = 64.130 \text{ Volts}$$

c) Unit Peak Width,  $\Delta M = 1.00$  amu

$$V_{in(MAX)} = \frac{1.00}{1.32} (47.030) = 35.629 \text{ Volts}$$

Maximum Inlet Aperture For 100% Transmission:

a) Design Goal Instrument,  $\Delta M = 1.32$  amu

$$D_{in} \cong 0.8 \frac{r_o}{\sqrt{M/\Delta M}} = 0.8 \frac{(0.41056)}{\sqrt{227.27}}$$
$$= 0.0218 \text{ cm} = 0.0086''$$

b) Worst Case Instrument,  $\Delta M = 1.80$  amu

$$D_{in} \cong \frac{\sqrt{227.88}}{\sqrt{166.67}} (0.0086'') = \frac{15.075}{12.910} (0.0086'')$$
$$= 0.0100''$$

Maximum Beam Half Angle For 100% Transmission:

a) Design Goal Instrument,  $\Delta M = 1.32$  amu

$$E_t \cong \frac{V}{30(M/\Delta M)} = \frac{1500}{30(227.27)} = 0.22000 \text{ Volt}$$

$$\tan \theta = \sqrt{\frac{E_t}{V_{in(MAX)}}} = \sqrt{\frac{0.22000}{47.030}} = 0.06839$$

$$\therefore \theta = 3^\circ 55' \cong 3.9^\circ$$

Since  $E_t$  and  $V_{in(MAX)}$  both vary directly with  $\Delta M$ , the value of  $\theta$  above holds for the worst case instrument with  $\Delta M = 1.80$  amu as well as for a unit peak width instrument with  $\Delta M = 1.00$  amu.

### Quadrupole Sweep Constants

$$U = a V - b$$

$$\begin{aligned}\Delta M &= 7.94 (0.16784 - a) M + \frac{1.10 b}{v^2 r_o^2} \text{ amu} \\ &= \Delta M_1 + \Delta M_2\end{aligned}$$

- a) Constant Peak Width Mode,  $\Delta M_2 = 1.32 \text{ amu}$ ,  $\Delta M_1 = 0$

$$a = 0.16784$$

$$\begin{aligned}b &= \frac{v^2 r_o^2}{1.10} \Delta M = \frac{(4.1090)(0.16856)}{1.10} (1.32) \\ &= 0.83115 \text{ Volt}\end{aligned}$$

- b) Hybrid Mode, assume  $\Delta M_1 = 0.42 \text{ amu}$ ,  $\Delta M_2 = 0.90 \text{ amu}$

$$\frac{0.42}{7.94(300)} = 0.167840 - a = 0.000176, a = 0.167664$$

$$b = \frac{0.90}{1.32} (0.83115) = 0.56669 \text{ Volts}$$

$$\Delta M = \frac{M}{300} (0.42) + 0.90 \text{ amu}$$

- c) Worst Case Hybrid Mode,  $\Delta M_1 = 0.90 \text{ amu}$   
 $\Delta M_2 = 0.90 \text{ amu}$

$$\frac{0.90}{7.94(300)} = 0.167840 - a = 0.000378$$

$$a = 0.167462$$

$$b = 0.56669 \text{ Volts}$$

$$\Delta M = \frac{M}{300} (0.90) + 0.90 \text{ amu}$$

### Ion Source Design

The exit cathode of the ion source was used to limit the maximum beam half angle  $\theta$ . The exit cathode first aperture had a diameter of 0.120 inch while the second aperture had a diameter of 0.060 inch and was spaced 0.945 inch away from the first aperture. The maximum direct beam half angle out of the ion source was

$$\theta_s = \tan^{-1} \frac{.09000}{.94500} = \tan^{-1} .095238 = 5^\circ 26'$$

The half beam angle of the ions actually entering the quadrupole depended on the diameter of the quadrupole entrance aperture and its spacing from the first aperture. Since the quadrupole entrance aperture diameter was 0.100 inch and its spacing from the 0.120 inch diameter ion source aperture was 1.240 inches, then the ion beam half angle was

$$\theta = \tan^{-1} \frac{.11000}{1.2400} = \tan^{-1} .088710 = 5^\circ 4'$$

If the entrance aperture diameter of the quadrupole were .060 inch, the ion beam half angle  $\theta$  would be  $4^{\circ} 9'$ , just about matching the maximum beam half angle of  $3^{\circ} 55'$  required for 100% transmission.

The maximum energy of ions that leave the ion source was measured at different pressure levels and was found to vary from 74 electron volts for a pressure of  $2 \times 10^{-8}$  Torr to 40 electron volts at  $7.8 \times 10^{-5}$  Torr for nitrogen gas. If the axial ion energy was to be kept below 35 volts so that peak widths approaching 1.00 AMU were not limited by axial ion energy, retardation of the ions was required. Retardation caused some defocussing so that the amount of retardation used was determined experimentally.

#### Multiplier Design

The major problem in designing an electron multiplier arrangement for a quadrupole mass spectrometer is to collect as many positive ions as possible and block or reject as many of the undesired photons as possible. The standard technique for solving this problem is to physically place the electron multiplier off-axis and then deflect the ions into the first dynode of the multiplier.

In order to simplify the construction of the RGA and keep the analyzer and multiplier cylindrically symmetric and "in-line", it was decided to leave the multiplier "on-axis". Because the first dynode entrance aperture was relatively large (.275" x .370"), it was possible to shield the central part of the first dynode from the analyzer-collimated photon beam and deflect the ion beam over to an open end portion of the first dynode.



The exit aperture of the quadrupole was chosen so that the photon beam diameter defined by the entrance and exit apertures of the quadrupole analyzer was one third the width of the first dynode entrance aperture, or .123 inches wide, at the first dynode. Two thirds of the first dynode entrance aperture, including the central third, was shielded. It was then necessary to deflect the positive ion beam by a distance of .123 inch so it would enter the open third of the first dynode entrance aperture.

The design of the electron multiplier deflection plates assumed that the ions were deflected in a parallel plate capacitor, and that the deflection distance  $D$  from the axis was given by the equation

$$D = \frac{L' \ell}{2} \frac{V_d}{V_a} \quad (13)$$

where  $L'$  is the distance from the center of the deflecting plates to the first dynode,  $\ell$  is the length of the deflecting plates,  $d$  is the spacing between the plates,  $V_d$  is the potential difference between the plates (in volts) and  $V_a$  is the energy of the ions (i.e. the axial energy expressed in volts). One of the deflecting plates was kept at the full (negative) electron multiplier voltage while the other plate was maintained at a somewhat less negative potential that was a fixed fraction of the full multiplier voltage in order to create the potential difference  $V_d$ . The actual potential used was determined experimentally. The chief advantage of this arrangement was that the ion beam deflection  $D$  was independent of the multiplier voltage (and thus of the multiplier gain).

## Electronic System Design

The electronic system is composed of four basic units: sweep circuits, rf generator, electrometer and power supply. Two additional high voltage power supplies are also used but these are separate packages merely connected to the input lines. The system is designed to operate from a 28 vdc negative ground power source.

RF Generator. - A large portion of the package volume is devoted to the rf generator. The volume is required by the separate rf box shield which is necessary to prevent rf fields from interfering with the operation of the other electronic circuits. All leads into the box are by-passed by feedthrough capacitors to insure the integrity of the shielding enclosure.

The generator is a crystal controlled oscillator-power amplifier transmitter which will provide the 3000 volt peak to peak rf voltage to operate the quadrupole. The frequency is fixed by the crystal at 2 MHz. The oscillator is constructed on a small circuit board and mounted in a separate shielded enclosure inside the main generator enclosure.

The power amplifier transistors are mounted in a heat sink which is thermally connected to an outside bottom corner of the main package so that external heat sinking may be attached to the bottom of the package, to which is also mounted the power supply transistor heat sink. Tuning of the power amplifier

is provided by two piston capacitors so that rf voltage balance can be obtained with minimum capacity added to the quadrupole capacity. These capacitors are accessible thru the top of the rf enclosure. The output circuit return is grounded only at the quadrupole to prevent rf ground loops and consequent instabilities.

Sweep Circuits. - The sweep circuit board includes these functions; ramp generator, plus and minus dc rod voltages, and rf modulator. The sweep ramp generator is a capacitor charging ramp in the feedback loop of the plus dc amplifier. The ramp is automatically reset when the sweep reaches approximately mass 150 or mass 300 if the external mass range lead is grounded. The minus dc is derived from the plus dc by a similar but inverting amplifier.

The modulator is an operational amplifier which maintains the rf amplitude at a fixed ratio to the dc voltage. The diode detectors in the rf generator sample the rf amplitude and thus dc voltage is returned to the turning point of the op-amp along with the +dc rod voltage. A small fixed voltage is also introduced to provide the "b" term for the constant peak width mode of operation (see equation 11).

Electrometer. - The linear electrometer provides automatic range changing over four decades. The lowest range is  $10^{-9}$  amps full scale. Range changing is provided by MOSFET transmission gates which are triggered by an up/down counter which is driven by two (high and low) comparator circuits. An internal 10 KHz clock provides the timing for the range changing circuits.

The electrometer amplifier incorporates a MOSFET input stage and an IC op-amp with a feedback loop including the range resistor. A ten volt output represents the top of each range. The overrange comparator is set to trigger the counter at 10 volts and the under range comparator is set at .8 volts. A varying input signal passing through either of these set points will trigger on up or down count of the counter to change range as required. The counter is inhibited for counts beyond the four ranges available. Range information is taken from the binary output of the counter.

A dc to dc converter is included at the output of the electrometer to provide an isolated signal output circuit.

Power Supply. - The power supply includes an input switching regulator and a dc to dc converter which supplies the required voltages. The two low voltages (plus and minus 13V) are regulated with IC regulators. The higher voltages (plus and minus 300 V and 140 V) are not separately regulated since the circuits in which they are used are essentially self regulated through feedback.

The quadrupole electronics operate with a mass zero power of 9.8 watts and a mass 300 power of 57 watts peak at 28 volts dc input. The average power required at 28 volts is about 38.5 watts.

## SYSTEM CONSTRUCTION

The three major subassemblies of the RGA, namely the ion source, analyzer and detector were designed to initially contain elastomer O-Ring type flanges so that they could be conveniently assembled and disassembled during the development and test phase of the program. After testing, the temporary flanges were machined off and the three subassemblies were welded together. A permanent metal O-Ring flange was used at the detector so that the electron multiplier could be changed conveniently at any time.

The RGA source, analyzer and detector had a cylindrical, "in-line" structure as shown in Figure 2. The analyzer was the largest component, being 2 inches in diameter and approximately 9 inches long. The length of the detector was about 6 inches while the length of the ion source was about 3 inches. The two tubulations which allowed gas to enter the ion source were located perpendicular to the longitudinal axis of the instrument as was the analyzer tubulation used to evacuate both the analyzer and the detector.

The construction of the ion source is shown clearly in the assembly drawing of Figure 3. The ion source was designed to use a perforated cylindrical anode that would permit gases to enter the source ionization region through either of the two transverse permanent entrance tubulations. For development and test purposes, the two transverse entrance tubulations were blanked off and the source was connected to a vacuum test system via a temporary Conflat flange located at the axial end of the source. The entrance cathode pole piece (subassembly 6 in

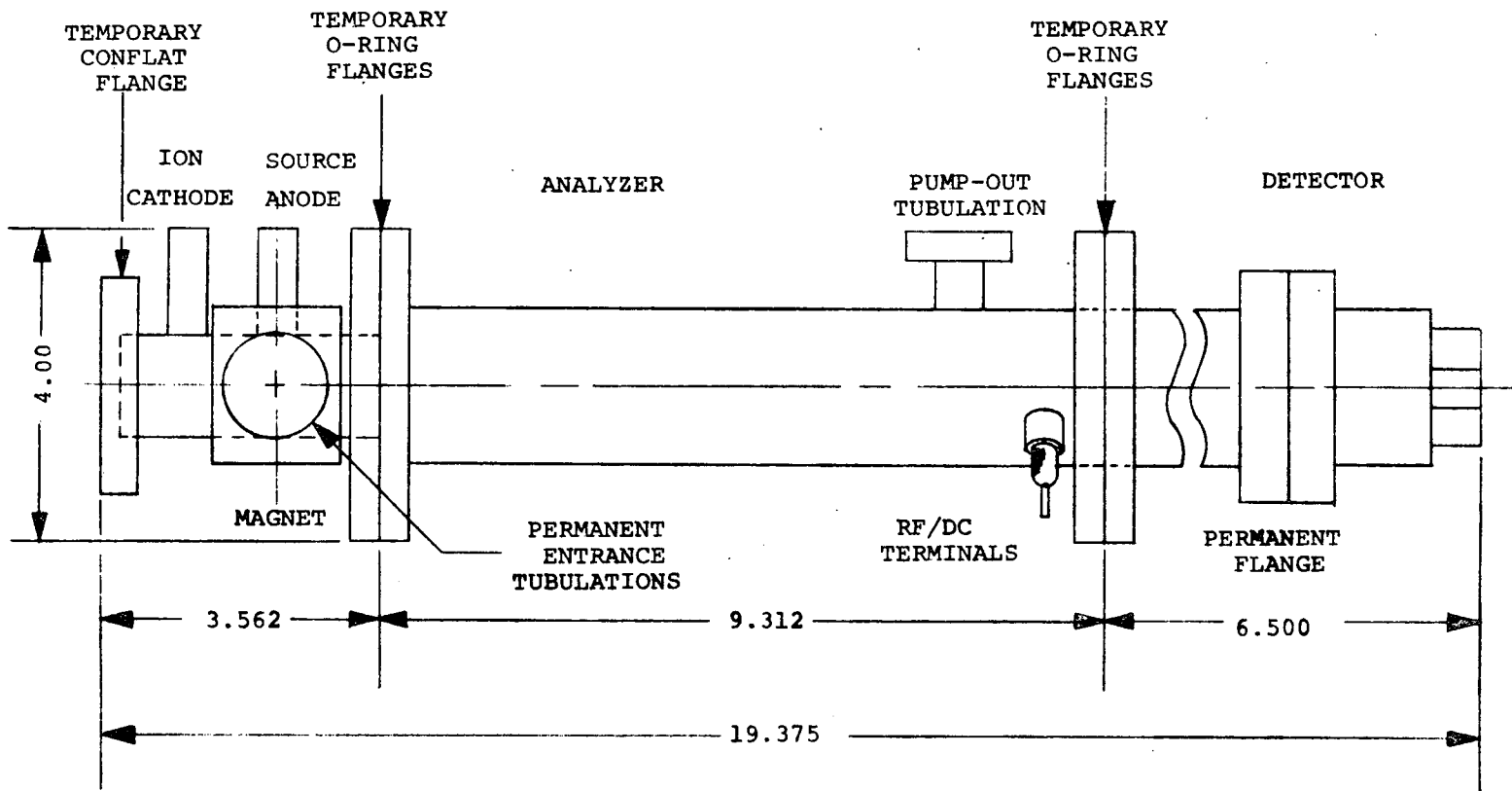


FIGURE 2. - PROTOTYPE RGA WITH TEMPORARY FLANGES

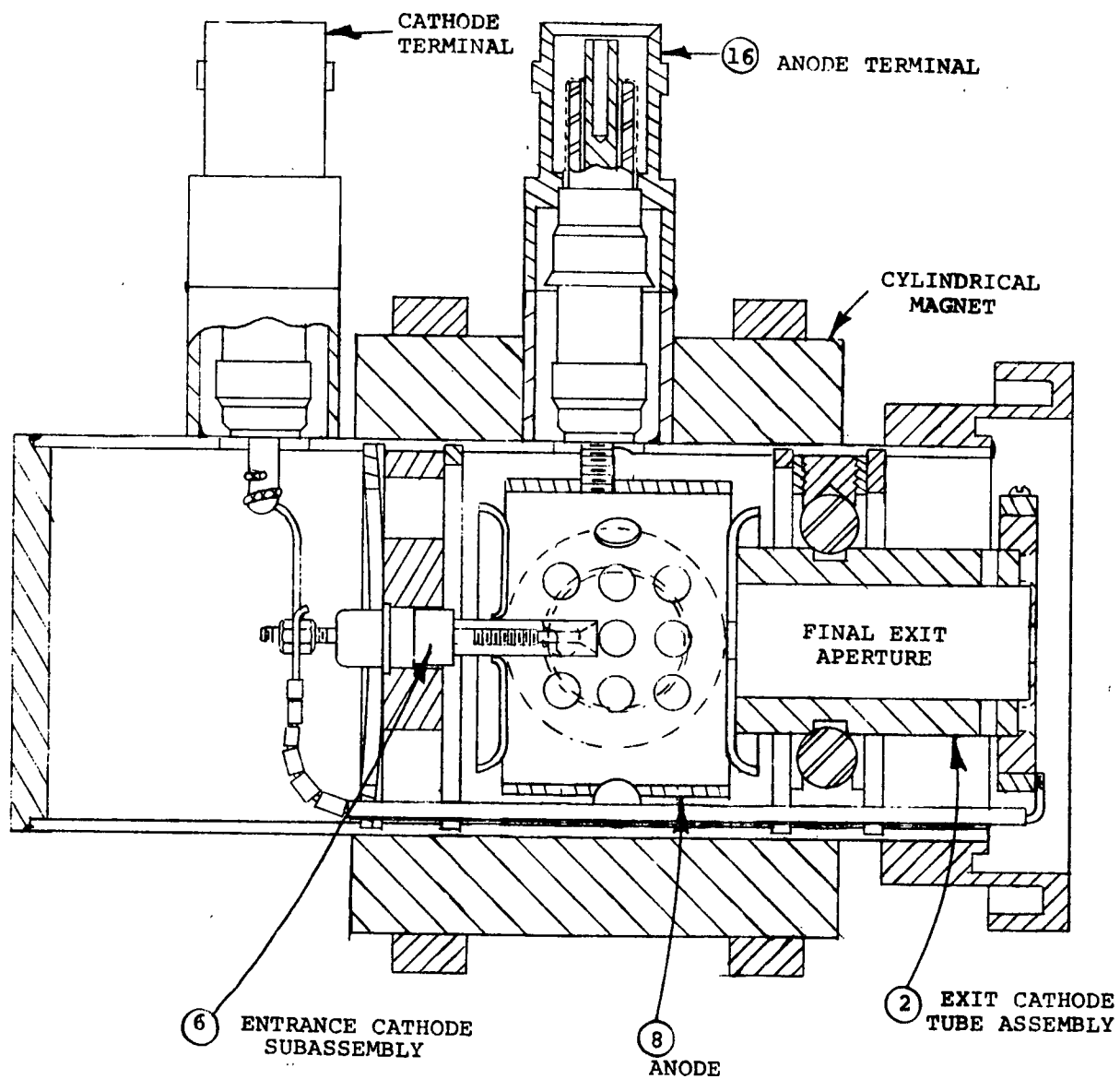


FIGURE 3. - CONSTRUCTION DETAILS OF THE RGA COLD CATHODE ION SOURCE

Figure 3) was perforated to permit gases to enter the ionization region from the test system. A special test flange (O-ring sealed) was designed and built to seal off the open, ion exit end of the source and allow ion currents and ion energies to be measured independent of the quadrupole analyzer. This test flange will be described in a later section.

The key elements of the cold cathode ion source were the cylindrical anode (8) and the disk-shaped cathodes (6) that closed off the open ends of the anode. The entrance cathode had a short, small diameter, cylindrical stub attached to it which extended half way toward the opposite exit cathode. This stub permitted a radial, "magnetron-like" discharge to be established between the anode and the cathodes. The exit cathode had a central aperture which allowed positive ions to leave the discharge region and travel through the exit cathode tube assembly (labelled 2 in Figure 3). A final aperture in the end plate of this assembly collimated the ion beam and thus formed an ion beam that would be compatible with the quadrupole analyzer.

The exit cathode assembly and the anode were supported mechanically by sapphire spheres located between the outer periphery of these elements and the ion source housing. The spheres also provided a high degree of electrical insulation. The entrance cathode was supported mechanically (and electrically insulated also) by a ceramic-metal feedthrough. The two cathodes were joined together electrically and connected to one BNC type vacuum feedthrough. The anode was connected electrically to a second BNC type vacuum feedthrough (item 16 in Figure 3). A cylindrical or sleeve type permanent magnet that was cut in half longitudinally was clamped around the outside of the ion source housing to provide the required axial magnetic field.



The magnet contained three clearance holes for the two entrance tubulations and the anode feedthrough.

As can be seen from Figure 3, both subassemblies were held in position with retaining rings. The two BNC feedthroughs were welded to short cylindrical mounting tubes that had been high temperature brazed to the housing with gold-nickel eutectic alloy. The two entrance tubulations were also brazed to the housing with gold-nickel eutectic alloy.

The construction of the quadrupole analyzer is shown in detail in Figure 4.

The analyzer consisted essentially of four rods 8 inches long which were spaced apart with high precision. Two sets of rods were fabricated for this program. One set had an approximate hyperbolic surface formed by a series of circular arcs. The second set of rods had a round cross section. The rods were fastened to four machinable ceramic spacers which permitted the rod positions to be adjusted to obtain a uniform inscribed circle of radius  $r_0$  between the rods surfaces over the length of the rods. The rods were fabricated from 316 SS for high strength and low creep rate.

The rod and spacer assembly was mounted within the analyzer housing by placing the assembly in axial tension rather than under axial compression, which tends to bend or bow the rods. Entrance and exit aperture plates were mounted within the analyzer housing approximately 0.100 inch from the ends of the rods. The exit aperture plate was fabricated in the shape of a hat with a series of holes in the cylindrical side wall to provide adequate vacuum conductance between the analyzer and the detector. Retaining rings were used to lock the aperture

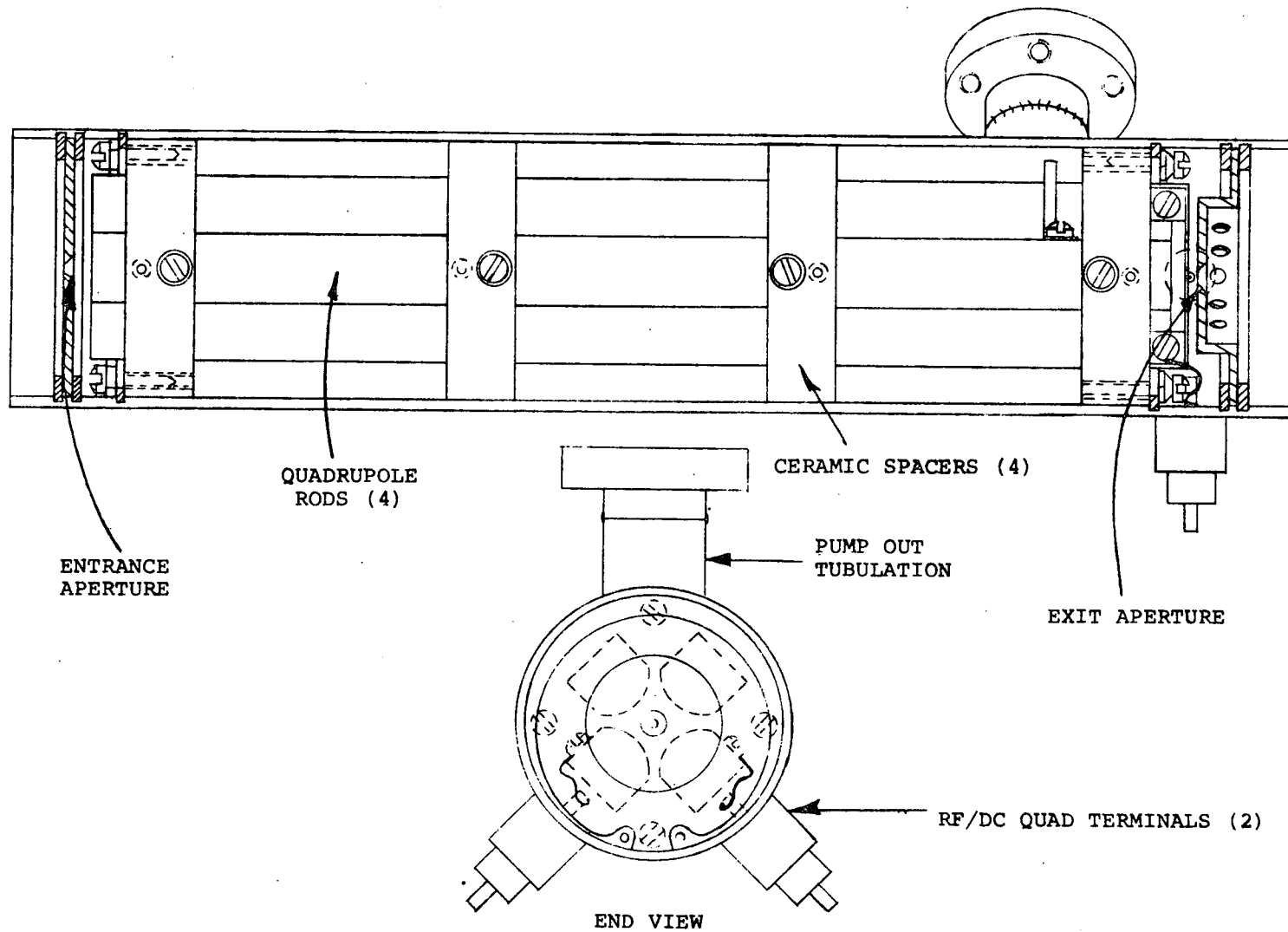


FIGURE 4. - CONSTRUCTION DETAILS OF THE RGA QUADRUPOLE ANALYZER.

plates in position and made it easy to change the aperture dimensions during development of the instrument. A 3/4 inch diameter side pumping tubulation (item 11 in Figure 4) was brazed to the analyzer housing near the end which joined the detector. This tubulation allows the analyzer and detector to be pumped out to a low background pressure. The two rf voltage feedthroughs were also located at the detector end of the analyzer. Opposite quadrupole rods were connected together electrically as required.

The construction of the RGA detector is shown in detail in Figure 5.

The heart of the ion detector was an EAI Model No. 974-0209 14 stage Be-Cu electron multiplier (11). The multiplier was mounted so that the center of the first dynode aperture was on the axial centerline of the instrument. The multiplier was modified by covering 2/3 of the first dynode aperture with a sheet of thin tantalum in order to block the central beam of photons from the ion source and analyzer. Positive ions from the analyzer were deflected toward the 1/3 open area of the first dynode aperture by installing two deflection plates above the top cap of the multiplier. One of the deflection plates was spot welded directly to the top cap and thus operated at the full negative potential of the multiplier. The second deflection plate (about 3/4 inch square and spaced about 3/4 inch from the first plate) was operated at approximately 60 percent of the full negative potential of the multiplier by connecting it electrically with a dynode that had that potential. A sleeve of aluminum oxide (labelled 2 in Figure 5) was used to electrically insulate the high voltage of the multiplier from the detector housing.

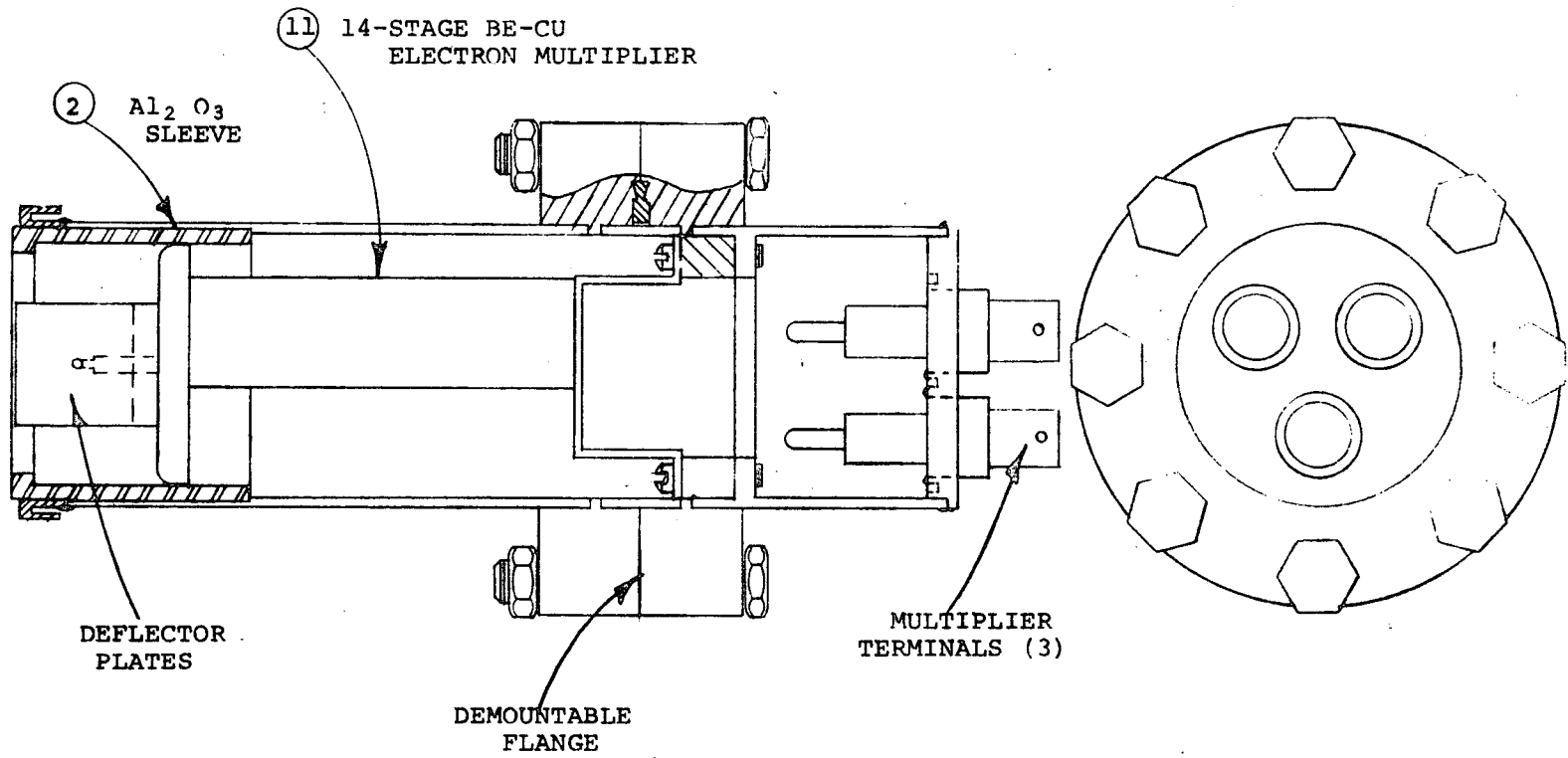


FIGURE 5. CONSTRUCTION DETAILS OF RGA DETECTOR.

Three BNC type vacuum feedthroughs were welded to the end plate of the detector. One of these feedthroughs was connected to the output electrode of the electron multiplier. The second feedthrough was connected to the internal resistor divider chain that furnished electrical potentials to all of the dynodes except the first dynode. The third feedthrough was connected to the first dynode.

In normal operation, the second and third feedthroughs were connected together externally with a shielded cable which also connected to the multiplier high voltage power supply. When the relative gain of the multiplier was to be measured, the positive ion current to the first dynode and top cap was measured by connecting an electrometer to the third feedthrough.

Special Conflat type flanges were used to provide demountability for the electron multiplier. In this way, the multiplier could be easily cleaned or replaced.

It was found advantageous to coat the multiplier top cap and deflection plates with a layer of aquadag (colloidal carbon in an aqueous solution) in order to reduce photon scattering in this region and thus lower the undesired photon background.

The design of the total package that contained the electronics and held the analyzer is shown in Figure 6.

## DEVELOPMENT AND TEST RESULTS

### Ion Source

The completed ion source was tested by itself to determine its sensitivity and ion energies for nitrogen gas over a range of pressures from  $10^{-8}$  to approximately  $10^{-4}$  Torr. In

Reproduced from  
best available copy.

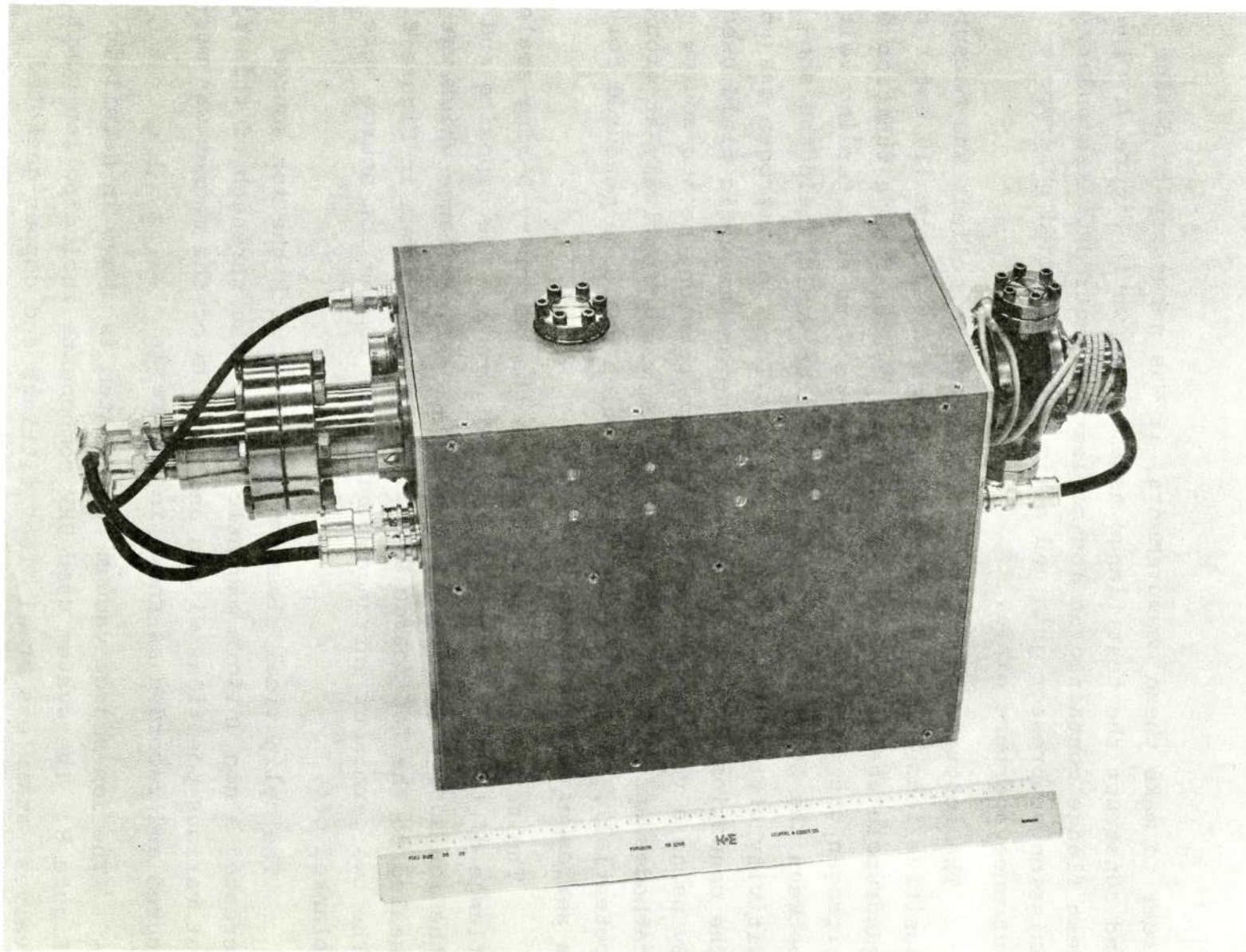


FIGURE 6. - PHOTOGRAPH OF LABORATORY PROTOTYPE RGA.

order to make these measurements, it was necessary to design and construct the test flange assembly shown in Figure 7. The test flange contained an ion collector electrode, a secondary emission suppressor grid and a simulated grounded quadrupole entrance aperture plate.

The function of the test flange was to collect and measure positive ions from the ion source which would normally enter the quadrupole analyzer. The ion current measured as a function of nitrogen gas pressure in the ion source with no retarding voltage between the source and the ion collector would yield the sensitivity of the ion source in amperes/Torr for nitrogen gas under the conditions of source anode voltage and magnetic field used. By using a variable retarding voltage between the ion source cathodes and the ion collector (which was effectively at ground potential), the ion energy distribution would be measured for a series of nitrogen gas pressures.

The test flange was bolted to the temporary O-ring-sealed flange of the ion source shown in Figure 2. The opposite end of the ion source contained a temporary Conflat flange which was sealed to the Ion Source Vacuum Test System shown in Figure 8. The two permanent entrance tubulations of the ion source were blanked off.

The cylindrical sleeve magnet used with the ion source created a non uniform magnetic field. The strength of this field at various positions within and outside of the magnet was measured and recorded as shown in Figure 9.

The ion source vacuum test system is shown in detail in Figure 8. The system used UHV components including ion pumps, valves, stainless steel "Tee" fittings and copper-gasketed Conflat flanges. A glass envelope Bayard Alpert gauge was used

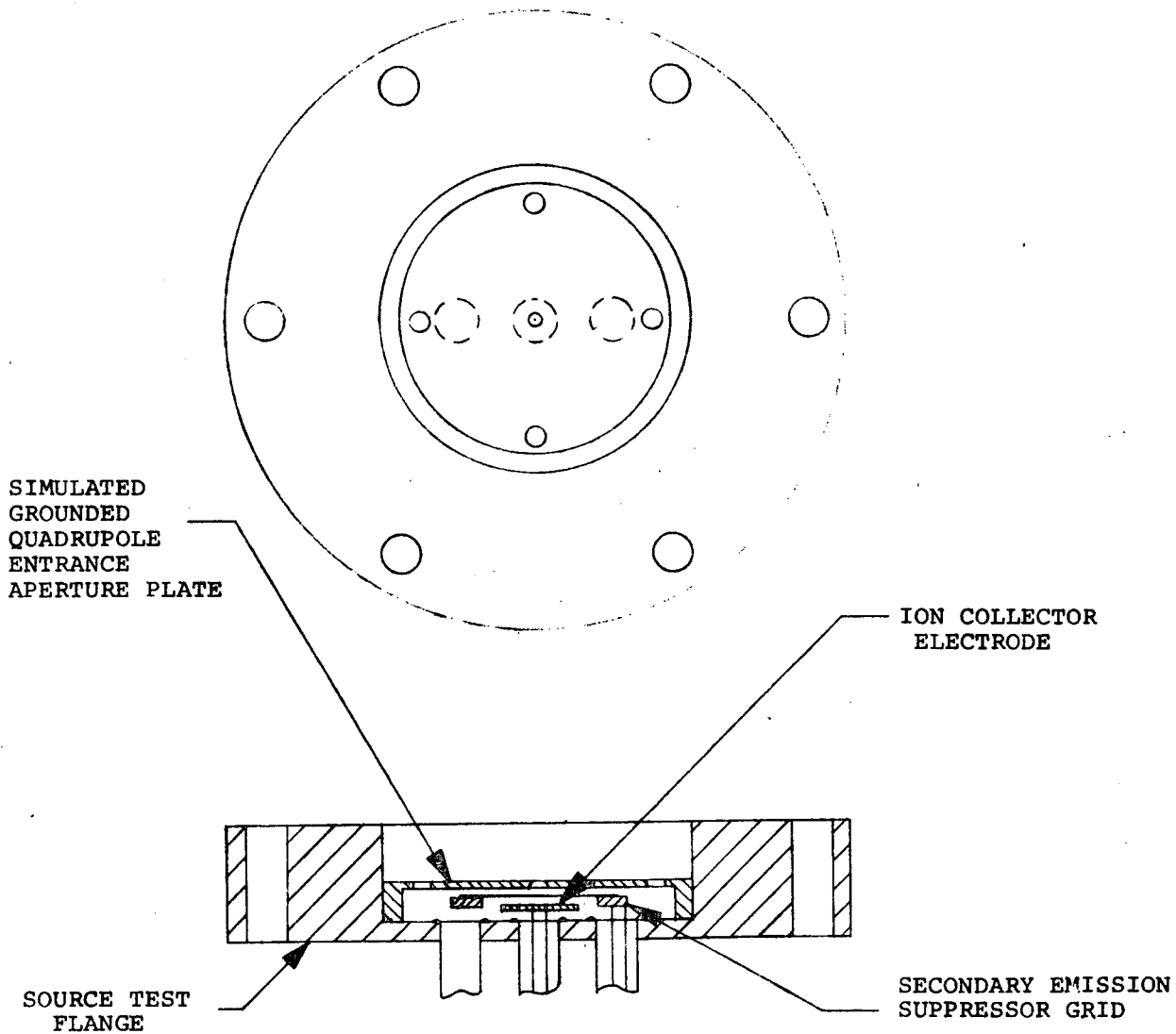


FIGURE 7. - PROTOTYPE RGA ION SOURCE  
 TEST FLANGE ASSEMBLY.



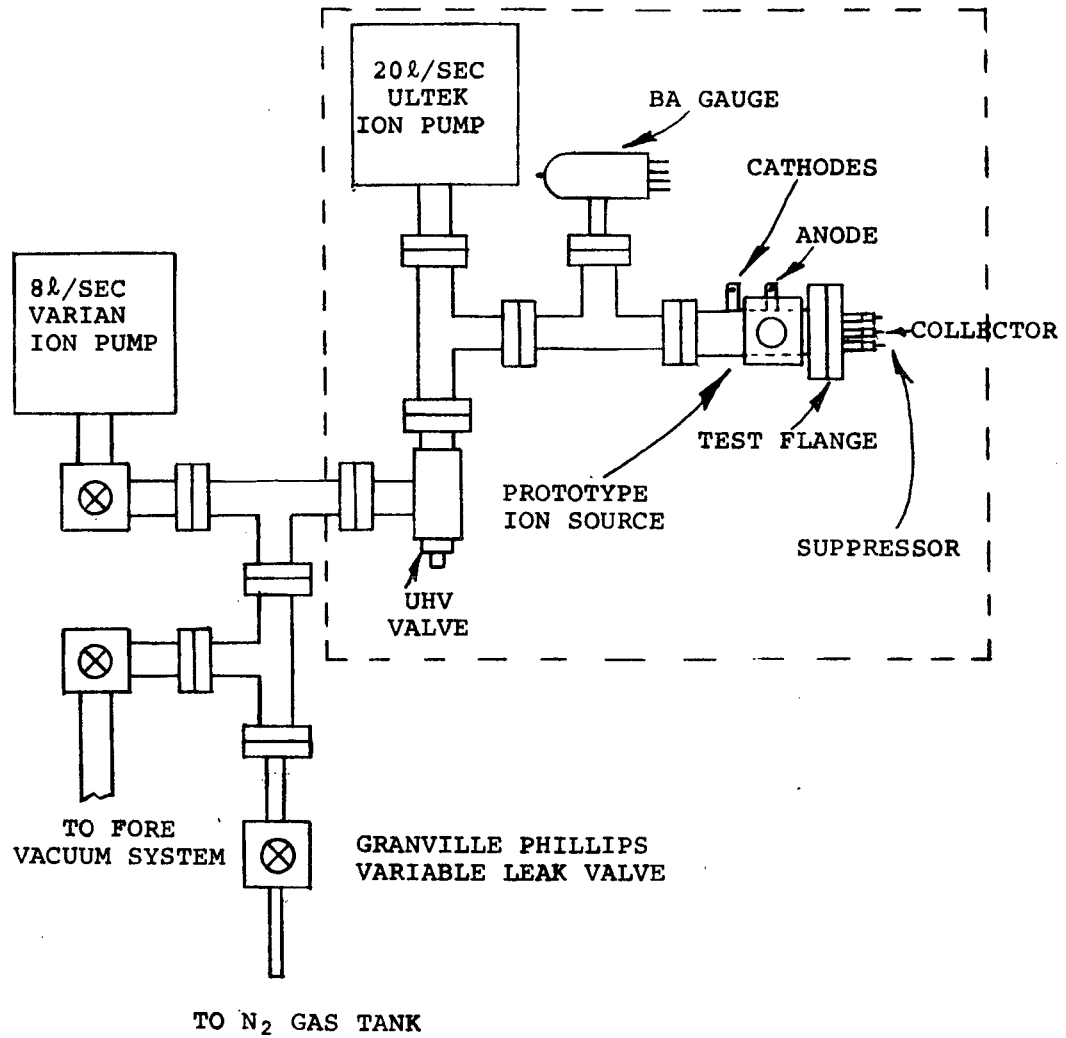
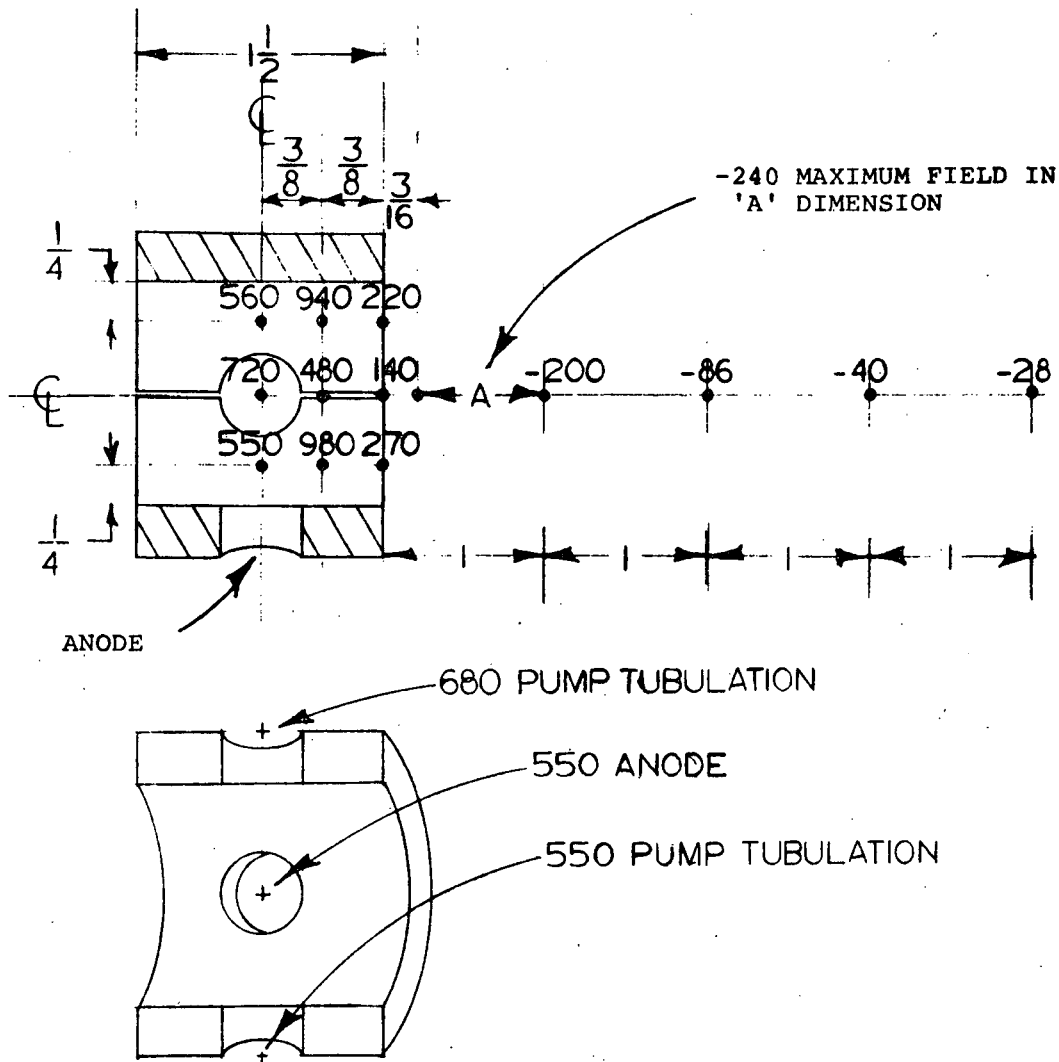


FIGURE 8. - PROTOTYPE RGA ION SOURCE VACUUM TEST SYSTEM WITH INSTALLED ION SOURCE AND TEST FLANGE



**NOTE:**

- (1) The cathode pole pieces increase the magnetic field in the region of the ion source discharge and may decrease the fringe field.
- (2) All magnet field valves in oersteds.

**FIGURE 9. - MAGNETIC FIELD STRENGTHS WITHIN AND OUTSIDE THE ION SOURCE CYLINDRICAL MAGNET.**

to measure the system total pressure. The high vacuum upper portion of the test system was supplied with an oven and temperature controller that permitted the main 20 liter/sec ion pump, the Bayard Alpert gauge and the prototype RGA Ion Source to be baked out. Pure nitrogen gas was admitted to the system via a Granville Phillips variable leak valve.

After the ion source was installed on the test system and pumped down, the upper part of the system was mildly baked at 125°C. The total background gas pressure in the test system after this procedure was about  $2 \times 10^{-8}$  Torr as measured with the Bayard Alpert gauge. It was assumed that permeation and outgassing of the Viton O-ring in the test flange seal was one of the elements limiting the background pressure.

The equipment and electrical connections that were used to measure ion energies are shown in Figure 10. The ion collector electrode of the test flange was connected through an electrometer to ground so that its potential was essentially ground potential. The suppressor grid electrode was connected to a source of negative potential. It was found that a suppressor grid potential of -100 volts was effective in returning all of the secondary electrons emitted by the collector. The ion source anode voltage was supplied through a battery operated electrometer by a regulated power supply set for 1000 volts. The potential of the ion source cathodes was varied with a digital output, highly regulated power supply.

Ion source current sensitivity and ion energy measurements were made by first establishing a constant nitrogen gas pressure in the test system as indicated by the Bayard Alpert gauge and

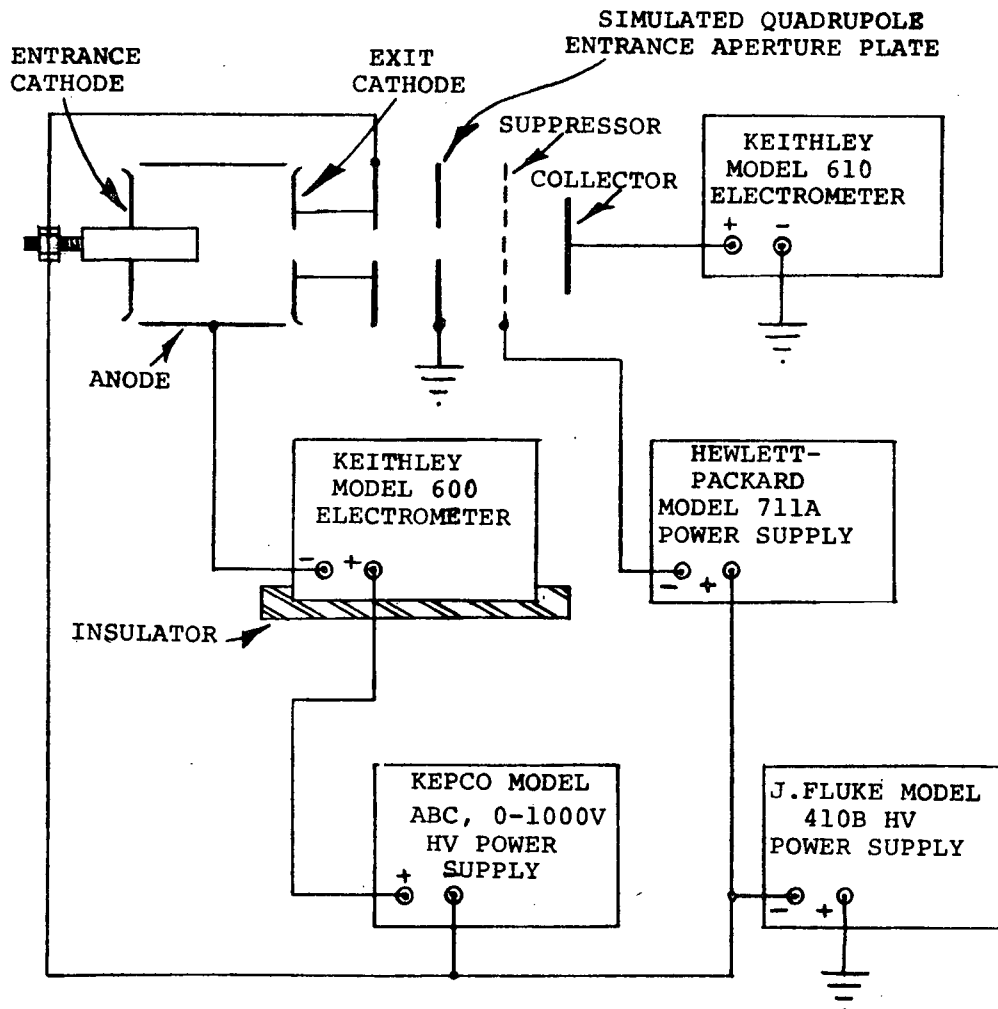


FIGURE 10. - EQUIPMENT AND ELECTRICAL CONNECTIONS USED TO MEASURE ION ENERGIES.

the battery operated electrometer which measured the total discharge current in the ion source and was thus a measure of the total pressure in the ion source. The sensitivity of the ion source was equal to the measured ion collector current with the source cathodes at zero or ground potential. Ion energies were measured by using the standard retarding potential method in which the ion source cathodes were made progressively more and more negative in steps of 1 or 2 volts. The ion collector current was recorded for each value of cathode potential until the collector current decreased to zero. The data were plotted as fractional cumulative positive ion current as a function of ion energy. The cumulative curves were numerically differentiated to yield a normalized positive ion current per energy interval. Typical smoothed ion energy curves are shown in Figure 11.

Summarizing the results of the ion source tests, it can be said that the source operated smoothly over the nitrogen pressure region from  $2 \times 10^{-8}$  Torr to about  $2 \times 10^{-4}$  Torr, with no evidence of mode changes. Ion energies ranged out to 64 eV at  $7.60 \times 10^{-8}$  Torr  $N_2$  and decreased steadily as the pressure increased, so that the maximum ion energy at  $7.80 \times 10^{-5}$  Torr  $N_2$  was 40 eV.

The total current sensitivity and the extracted ion current sensitivity for nitrogen gas are shown as functions of pressure in Figure 12. The total current sensitivity was about 1.0 ampere/Torr while the extracted ion current sensitivity seemed to vary from about  $1.5$  to  $2.0 \times 10^{-5}$  ampere/Torr.

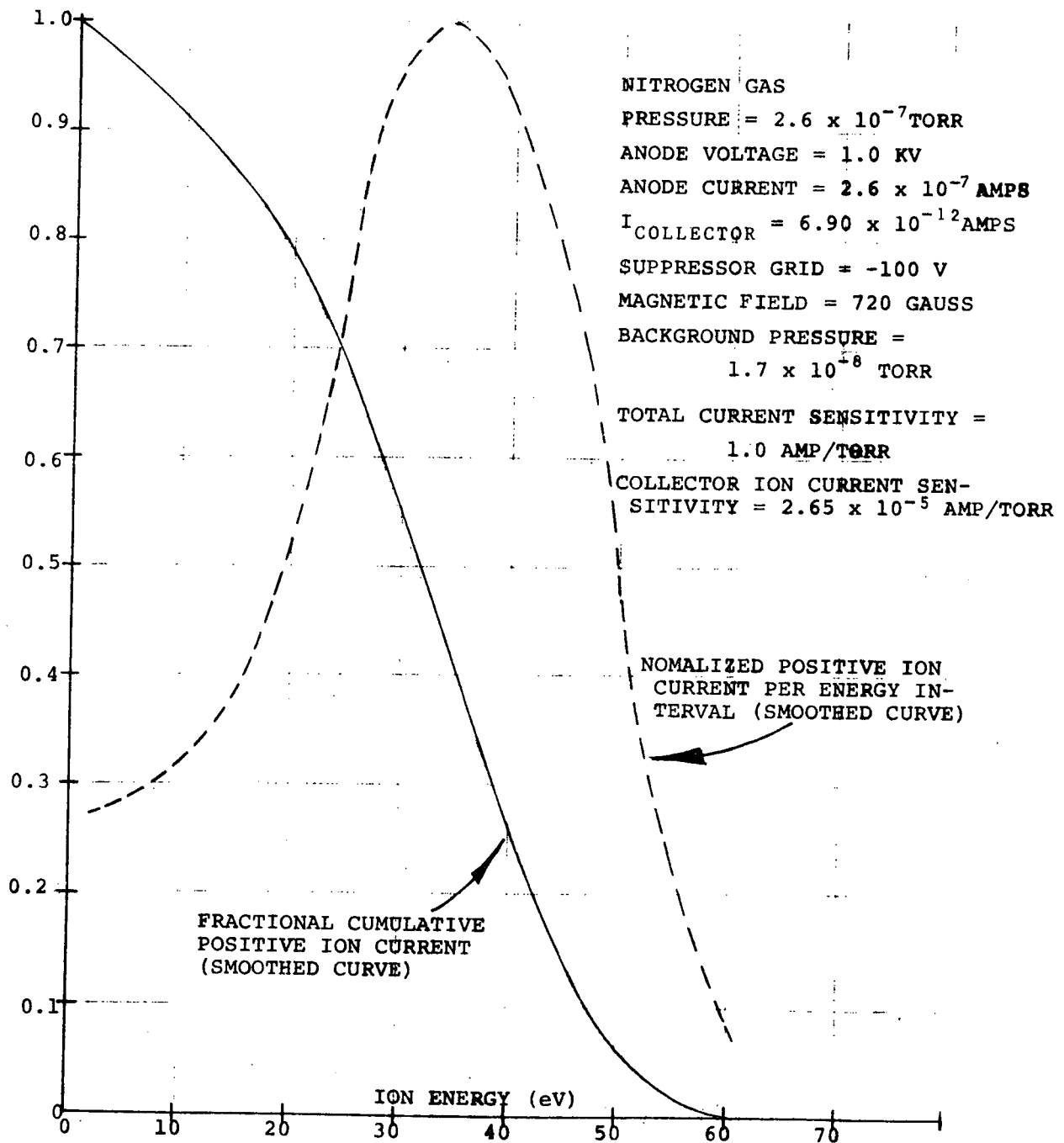


FIGURE 11. - PROTOTYPE RGA ION SOURCE ENERGY DISTRIBUTION.

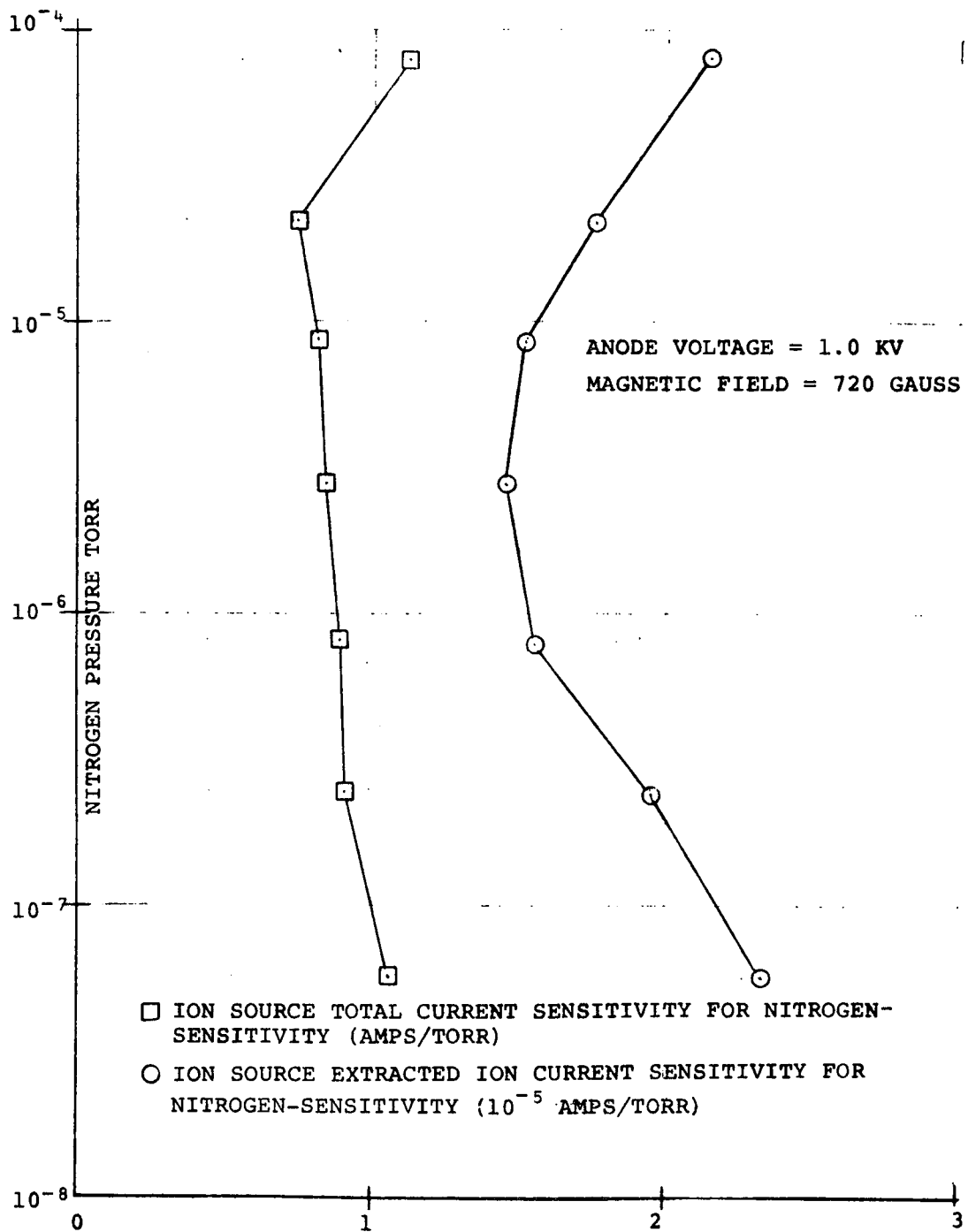


FIGURE 12. - PROTOTYPE ION SOURCE SENSITIVITY CURVES FOR NITROGEN GAS.

## Quadrupole Analyzer

The complete analyzer assembly (ion source, quadrupole and electron multiplier) was attached to a small, ion-pumped vacuum system for preliminary testing. The immediate goal was to determine the maximum resolving power obtainable using the hyperbolic rod analyzer. An EAI Model 200 quadrupole rf/dc sweep generator was used to supply the operating voltages for the quadrupole. The rf frequency of this sweep generator was 1.65 MHz; slightly below the design value of 2.0 MHz specified previously. At this frequency, the sweep generator will scan a mass range up to approximately 290 amu with the hyperbolic rod analyzer.

To test the instrument at these high mass numbers a sample of tungsten hexafluoride\* gas was introduced, along with a mixture of all the inert gases (except radon) and the system residual gases.

The sweep electronics was adjusted to yield the maximum resolving power near 281 amu (the last mass peak in the tungsten hexafluoride series). The maximum resolving power obtained at this time was such that the valley between two peaks of nearly equal height, separate by 2 amu (279 and 281) was about 50%. This is less than the minimum design goal value for  $\Delta M$  of 1.8 amu. Therefore, a systematic experimental study was undertaken to determine if improvements could be made.

A number of variables are known to effect the resolution performance of the quadrupole analyzer. Among these are:

---

\* This material and its mass spectrum are discussed on pp. 59-61.



Ion Energy (axial and transverse)

Entrance Angle

Frequency

Mechanical Tolerances

Electrical Tolerances

RF and/or DC Voltage Balance

Exit Aperture Diameter

Each of these variables was examined carefully either before mechanical assembly or during a specific set of tests. For example, four entrance aperture diameters (.008, .030, .060 and 0.119 inches) and two exit aperture diameters (.059 and 0.100 inches) were studied. The frequency was also increased from 1.65 MHz to 1.87 MHz). Ion energy was studied using two methods of retardation and also by reducing the anode voltage on the cold cathode ion source. Both the rf and dc quadrupole voltages were carefully balanced and the linearity of the U/V ratio was also checked. None of these variables produced any significant improvement either individually or in consort with the others. It was found, however, that improving the ground connections from the sweep generator to the analyzer did increase the resolving power slightly throughout the overall mass range. This improvement still did not permit the original design goals to be met, however. The maximum resolution attainable using the hyperbolic rod analyzer was such that a valley of approximately 33% of peak height was observed for two nearly equal peaks spaced two amu apart. It is presently believed that mechanical tolerances limited this maximum resolving power. Possibly the accuracy of the hyperbolic surface limited the resolution, since great care was taken to maintain  $r_0$  to a few ten-thousandths of an inch.

It was decided to substitute the rod-round analyzer and to compare its resolving power with that of the hyperbolic unit. The results were definitely superior to those obtained from the hyperbolic analyzer. Peak-to-valley ratios of 10:1 (10% valley) or better were obtained where formerly the limit was 3:1. Again, these figures are for two peaks two amu apart and of nearly equal height.

In summary, the round-rod analyzer yielded superior resolution performance despite the fact that the hyperbolic rod section is known to be theoretically capable of higher performance than rod round units. It is speculated that the accuracy of the hyperbolic section may be the root cause of the problem. The final assembly of the analyzer was made using the round-rod analyzer. The round rod analyzer was found to be more favorable from the electronics standpoint because of its lower rod capacitance. As equation (1) shows, this has a salutary effect on rf power.

#### Electron Multiplier

The electron multiplier detector was not tested separately but was tested in combination with the ion source and analyzer. The electron multiplier was operated with voltages ranging between -1.0 and -2.5 KV and appeared to have its nominal gain judging from the ion source pressure and output current values.

One of the earliest tests made with the electron multiplier was an attempt to block the central photon beam, as defined by the entrance and exit apertures of the quadrupole analyzer, and

still collect a majority of the positive ions without the use of a deflecting electric field. Theory indicates that ions exiting from the quadrupole can have a large transverse energy and thus should form a wide angle beam. The results of the test, however, indicated that the exiting ion beam was approximately the same width as the photon beam, at least when the entrance and exit apertures of the quadrupole were equal and small (.060" diameter). This particular photon blocking scheme did not improve the signal to noise ratio, but only succeeded in reducing the signal level by about two decades.

The signal to noise ratio of the electron multiplier was increased significantly by a factor of about 15 by moving the electron multiplier further away from the exit aperture of the quadrupole, blocking the central part of the first dynode area where the photon beam impinged, and providing parallel deflecting plates to deflect the ion beam over to one edge of the first dynode. This signal to noise ratio was further improved by blackening the deflection plates, the top cap of the multiplier including the photon blocking strip and the exit aperture of the quadrupole. Aquadaq was used to provide the conducting black layer.

The voltage for the ion beam deflecting plates was obtained from one of the dynode resistors. A voltage of about 60 percent of the full negative multiplier voltage was found to provide optimum deflection of the ion beam.

The only experimental difficulty encountered using the multiplier was a noticeable loss in gain, believed to be the result of exposure to the test gas, tungsten hexafluoride. This

gas similarly "poisoned" a thoria-coated filament in the Bayard-Alpert gauge used to measure total pressure. Attempts were made to rejuvenate the gain of the multiplier by an overnight bakeout at 400°C. This technique has been used very successfully on low gain multipliers which have not been exposed to the tungsten hexafluoride. In this instance, however, the rejuvenation was not successful. A replacement multiplier was ordered to correct the problem. For this reason it is recommended the other gases be used in preference to  $WF_6$ .

### Electronic Development

The two major areas which needed attention for this project were the rf generator - to attain the high rf voltage required, and the linear electrometer - to switch ranges fast enough to follow the signal at the fast sweep rate required. Although higher dc rod voltages are also required high voltage transistors are available so that present techniques can easily be extended.

Rf Generator. - Calculations made using the physical parameters of the quadrupole indicated a required rf voltage of 3000 volts peak to peak. Assuming a  $Q$  for the output tank circuit of 200 and a quadrupole capacitance of 40 picofarads the generator would have to deliver a peak power of 22.8 watts.\* Previous experience indicated that at power levels above about 10 watts a ferrite core is not stable enough for high mass range quadrupole. For this reason an air core output tank coil was chosen. Again to meet the required stability, crystal control of the frequency is necessary.

---

\* Referred to output of rf tank circuit, not to 28 volt supply.

A crystal oscillator - power amplifier design was used in order to limit the loading of the crystal. Amplitude control is through the base bias of the oscillator stage. Maximum output voltage is more than 3000 volts peak to peak even with a finished quadrupole capacity of 38 pf.

The feedback rf detector for amplitude control became a problem when the system was integrated with the quadrupole. In order to obtain a small sample of the rf amplitude the detector diodes were driven from the collectors of the output transistors. (Loading of the full output tank was considered undesirable as a power drain.) It was determined that this drive point does not provide a true representation of the rf amplitude. Separate windings were added to the output coil to provide drive for the detector and the constancy of the U/V ratio was much improved. Further improvement was obtained by using diodes with a much faster reverse recovery time. The mass sweep now starts at mass 2 and the diode non-linearity is only apparent up to about mass 10.

Electrometer. - At the time this project was started NRC had been working on an all electronic automatic range switching electrometer for an in house project. The speed requirements were not as severe but the basic circuit problems had been solved.

Range switching is accomplished by means of MOSFET transmission gates with an open circuit impedance of  $10^{12}$  ohms. Switching sequence is obtained from a high point and a low point comparator and an up/down counter. The counter drives the transmission gates and provides the range information thru its binary output.

In the original electrometer, the counter was driven by a internal clock derived from the 60 cycle line (120 cycles). This of course, was much too slow for the present application. Increasing the clock frequency proved satisfactory up to about 1000 cycles but the response time of the electrometer itself became predominant.

In order to speed up the electrometer additional transmission gates were used to ground the open range resistor gates to essentially remove the range resistor capacity from the feedback loop. The circuit board was also redesigned to further isolate the input switching circuits from the output leads. These changes and some work on the comparators to reduce overshoot, finally permitted clock speeds of 10 kHz. The electrometer will now settle from a  $10^{-6}$  amp step in one millisecond on the up step and 1.6 millisecond on the down step (to below  $10^{-11}$  amps). This includes stepping thru the four ranges.

## OPERATIONAL CHARACTERISTICS

### General

This section of the report will describe and discuss the general operating characteristics and certain special features of the cold cathode residual gas analyzer. The operating characteristics such as resolution, sensitivity, mass range, dynamic range and S/N ratio will be described first in terms of actual test data obtained during laboratory tests of the instrument. Special features such as outgassing heaters, temperature monitors, mass range selection and multiplier gain measurements will be described thereafter.

## Operational Characteristics

The interpretation of mass spectra from any type of mass spectrometer is a very complex process requiring detailed analyses of each and every species encountered. Such effort is beyond the scope of the present contract work. Therefore, the reader is cautioned to exercise care in attempting to analyze the test spectra presented herein, particularly from the standpoint of peak height vs. partial pressure. The tendency to interpret large peaks of a given spectra as being the "major" constituents must be resisted until precision calibrations of both "major" and "minor" peaks have been obtained. In a previous section of this report,\* the variables affecting the sensitivity (peak height vs. partial pressure) of the instrument have been described and discussed. The combined interplay of these variables produces the observed sensitivity characteristic.

In a quadrupole analyzer, the adjustment of certain electronic parameters can lead to pronounced differences in the peak height vs. partial pressure relationship. It is entirely possible to adjust the so-called "a" and "b" terms in equations 10 and 11 so that the sensitivity for either low or high masses is emphasized by very large factors (greater than 10). This effect manifests itself in the spectra as noticeable differences in resolution (peak width) across the mass range. Since resolution and sensitivity are inversely related, the presence of very narrow peaks at one end of the

---

\*Refer to discussion on page 19.

mass range accompanied by much wider mass peaks at the other end signifies that the sensitivity (transmission) of the quadrupole is low within the region where very narrow peaks are observed. As explained previously, a hybrid mode of operation has been chosen wherein the peak widths vary slightly over the entire mass range. In this mode, the quadrupole resolution and sensitivity can be optimized as desired.

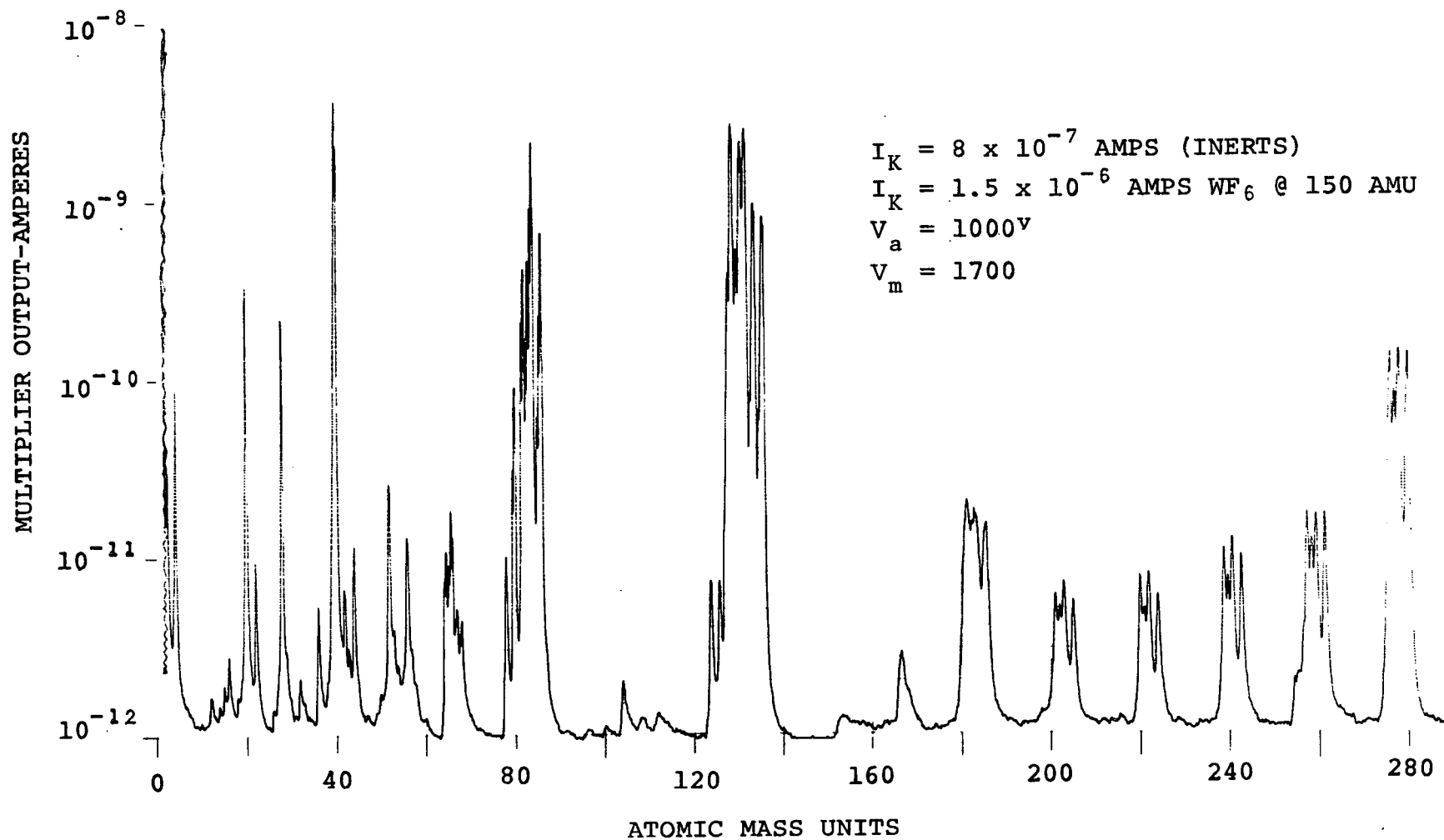
Figure 13 shows the performance of the instrument from 2-300 amu. These spectra were taken after introducing a mixture of the inert gases (helium thru xenon) together with an uncalibrated partial pressure of tungsten hexafluoride ( $WF_6$ ). System residual gases are also present in both major and minor amounts. It will be noted that the peak widths vary slightly over most of the mass range signifying that the quadrupole is operating in the hybrid mode discussed previously. The data shown in this figure were obtained using a laboratory logarithmic electrometer to show more clearly the large dynamic range of peak heights.

#### Discussion of Performance

Resolution. - Since the instrument is operating in the so-called hybrid mode, its ultimate resolving power ( $\frac{M}{\Delta m}$ ) must be determined near the highest mass measurable. For this purpose we refer to the last fraction observable for the tungsten hexafluoride series shown in Figure 13, namely  $(WF_5)^+$ . The parent molecular ( $WF_6$ ) is apparently fractionated



FIGURE 13. - SPECTRUM OF INERT GASES AND TUNGSTEN HEXAFLUORIDE AND SYSTEM RESIDUALS



completely by the ionization process and is therefore not observed. The four major peaks of the  $(WF_5)^+$  fraction occur at 277, 278, 279, and 281 amu.\* These are combinations of the four main isotopes of tungsten (182, 183, 184 and 186 amu) with five fluorine atoms. To simplify the resolving power determination, it is assumed that the basic peak shape is triangular (isosceles) and that the 279 and 281 peaks are of equal height. The valley between these peaks (280 amu) is 10% of either peak height after subtracting the photon background. With these assumptions it can be shown that the effective width of either peak at its base is approximately 2 amu at this portion of the mass range. The peak width measured near the two xenon isotopes, 134 and 136 amu, is obviously narrower since the valley between the peaks is about 3% of either peak. To provide acceptable values of sensitivity for the  $WF_6$  series, the resolution was not set to its maximum value. Hence the resolution performance noted in Figure 13 is less than the original design goal value.

Sensitivity. - An approximate sensitivity for the inert gases neon, argon, krypton and xenon was obtained in the following manner. The instrument's partial pressure response was measured for pure argon by admitting it to the spectrometer after a thorough evacuation of the instrument and the associated vacuum system. Pressure is measured by a Bayard-Alpert gauge (BAG) whose sensitivity for nitrogen is known.

---

\* Refer to Table I for all masses associated with the tungsten hexafluoride spectrum.

TABLE I

TUNGSTEN HEXAFLUORIDE ( $WF_6$ )

|            |               |               |               |                |               |
|------------|---------------|---------------|---------------|----------------|---------------|
| $WF_6$     |               |               |               |                |               |
| $(WF_5)^+$ | 275           | 277<br>(86.4) | 278<br>(46.4) | 279<br>(100.0) | 281<br>(93.3) |
| $(WF_4)^+$ | 256           | 258<br>(12.2) | 259           | 260<br>(14.3)  | 262<br>(13.3) |
| $(WF_3)^+$ | 237           | 239           | 240           | 241<br>(12.9)  | 243<br>(12.0) |
| $(WF_2)^+$ | 218           | 220           | 221           | 222<br>(12.2)  | 224           |
| $(WF)^+$   | 199           | 201           | 202           | 203            | 205           |
| $W^+$      | 180<br>0.122% | 182<br>25.77% | 183<br>14.24% | 184<br>30.68%  | 186<br>29.17% |

NOTE: Figures in parenthesis represent peak heights for the ten largest peaks relative to the highest peak (279 amu).

The percentage figures for tungsten represent percentage abundance of the isotopes.

(From "Compilation of Mass Spectral Data" by A. Cornu and R. Massot. Heydon & Son, Ltd., 1966.)

The sensitivity of the BAG for argon is derived from the nitrogen sensitivity using the data given by Redhead (Ref. 2) in Table 7.2 for the Ar/N<sub>2</sub> sensitivity ratio for a similar BAG. The BAG can then be corrected to read true pressure argon equivalent, provided argon is the predominant gas. This fact was demonstrated by obtaining a spectra similar to that shown in Figure 14. In the actual calibration run the true argon pressure was determined to be  $1.48 \times 10^{-6}$  Torr. The peak height at mass 40 was measured as  $5 \times 10^{-9}$  Amperes. Thus, the argon sensitivity was

$$S_A = \frac{5 \times 10^{-9}}{1.48 \times 10^{-6}}$$
$$= 3.38 \times 10^{-3} \text{ Amperes/Torr}^*$$

This sensitivity was obtained with an electron multiplier voltage of 2000 volts.

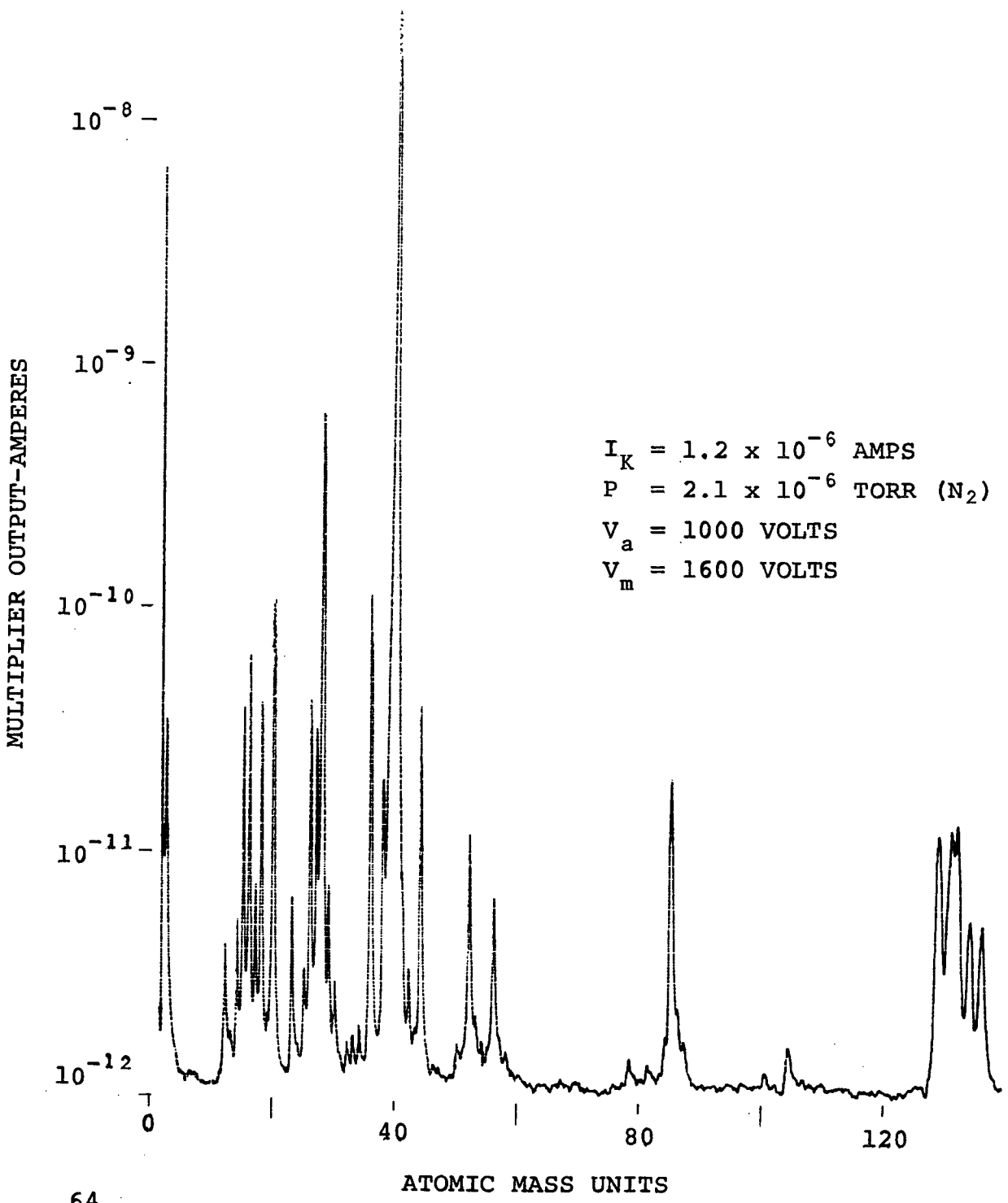
After determining the argon sensitivity, the sensitivities for all the inert gases were obtained using a mixture of helium, neon, argon, krypton, and xenon which contained equal percentages of each inert. A spectrum was obtained (same multiplier voltage) with this mixture which is similar to that shown in Figure 13 except no WF<sub>6</sub> was present. Using

---

\*The Ar<sup>36</sup> and Ar<sup>38</sup> isotopes have been neglected because of their very small abundance.

$10^{-7}$  -

FIGURE 14. - SPECTRUM OF ARGON AND RESIDUALS



the argon sensitivity derived above, the true argon pressure of the mixture was determined to be  $5.3 \times 10^{-8}$  Torr (argon). Since the mixture contained equal percentages of all the inerts, the partial pressure of each gas constituent was  $5.3 \times 10^{-8}$  Torr.

Using the known isotopic abundances of the inerts, an approximate sensitivity vs. mass number relationship can be derived from mass 4 (helium) to mass 136 (xenon). This relationship is shown in Table II below:

TABLE II  
SENSITIVITY VS. MASS NUMBER  
FOR THE INERT GASES

| <u>Mass No.</u> | <u>Peak Ht. (Amps)</u> | <u>Sensitivity (A/Torr)</u> |
|-----------------|------------------------|-----------------------------|
| 4 (Helium)      | $1.15 \times 10^{-11}$ | $2.2 \times 10^{-4}$        |
| 22 (Neon)       | $4.1 \times 10^{-10}$  | $5.8 \times 10^{-3}$        |
| 40 (Argon)      | $1.8 \times 10^{-10}$  | $3.38 \times 10^{-3}$       |
| 84 (Krypton)    | $6.0 \times 10^{-10}$  | $1.98 \times 10^{-2}$       |
| 136 (Xenon)     | $6.2 \times 10^{-10}$  | $1.31 \times 10^{-1}$       |

(Background subtracted from mass 4 peak height.)

The sensitivity figures listed in Table II clearly show that the sensitivity of the instrument increases noticeably as a function of mass. It must be recalled, however, (from previous discussions) that the ionization efficiency of the ionizer also increases approximately as the atomic number (electrons/molecule) for certain species. Thus, the xenon sensitivity (relative to argon) should be about a factor of two higher. The tabular sensitivity for xenon is actually about thirty-eight times greater than that for argon. This is a result of having purposely adjusted the instrument to emphasize the sensitivity to masses greater than xenon, namely those included in the  $WF_6$  series. Since the sensitivity of the BAG for  $WF_6$  is unknown and since the relative abundance of each fractionated peak is also unknown, the true sensitivity of the RGA for any of the  $WF_6$  peaks is purely speculative. Rather than set the sensitivity too low above xenon, it was decided to emphasize the higher masses since the instrument is primarily designed for this portion of the mass range.

Each of the spectra presented herein was obtained using a logarithmic electrometer to display the full dynamic range available without automatic ranging between minor and major peaks. The linear, automatic ranging electrometer has a sensitivity limit of about  $10^{-10}$  amperes (10% of maximum full scale sensitivity). From the Table II sensitivity data, the minimum detectable partial pressure of the inert gases can be calculated. For xenon<sup>(136)</sup> The minimum detectable partial pressure is  $10^{-10}/1.31 \times 10^{-1} = 7.6 \times 10^{-10}$  Torr (Xenon 136) equivalent to a total pressure of xenon =  $7.6 \times 10^{-10}/.0887$  or  $8.56 \times 10^{-9}$  Torr. Similarly, the minimum detectable partial pressure of helium is  $1 \times 10^{-10}/2.2 \times 10^{-4} = 4.5 \times 10^{-7}$  Torr (helium).

Dynamic Range and Signal to Noise Ratio. - In each of the spectra presented, a small baseline current will be noted in certain regions of the mass range where no peaks are observed. This current is due to a small flux of photons which originates within the cold cathode ion source and is eventually detected by the electron multiplier. The entrance aperture of the multiplier has been located off-axis so that the multiplier does not view the discharge region of the ion source directly. Analogous background currents are observed in hot-filament ionizers. One very important difference exists however, between the hot filament and cold cathode ionizers with regard to this background current. In the hot filament ion source this background is independent of pressure since it is related to the electron ionizing emission current which is constant. In the cold cathode ion source this background current is dependent on pressure, because the total electron current in the source is pressure dependent. At very low (UHV) pressures, this photon background declines as the pressure is reduced, so that a useful signal-to-noise ratio (S/N) is still maintained. At higher pressures, a small background may be observed depending on the total discharge current. Since this current depends on the number of major peaks as well as their individual intensities, the maximum S/N occurs when only one species predominates. This is the case shown previously in Figure 14 where argon is the only major peak. From this figure the S/N ratio is approximately  $3 \times 10^4$  to 1. In the presence of a large number of peaks at relatively high total pressures, the photon background is only a few percent of the full scale peak intensity on the electrometer's most sensitive ranges.



Linearity. - The linearity of the ion source total ion current has been observed on numerous occasions for both nitrogen and argon gases over a pressure range of  $5 \times 10^{-8}$  Torr to  $1 \times 10^{-4}$  Torr. The linearity is determined by comparison to a BAG which is believed to be linear up to  $1 \times 10^{-4}$  Torr. No unusual behavior occurred except when the ion source became grossly contaminated with  $WF_6$ . In this case the ion source exhibited a large mode switch near  $5 \times 10^{-7}$  Torr and the problem was corrected by cleaning the source.

Mass Range. - The mass range scanned by the instrument is 2 to 300 amu. The entire range is scanned in one continuous automatic sweep requiring approximately one minute per scan. Means have been provided for scanning only the 2 to 150 amu range should this be desired.

#### Special Features

A number of special features have been provided in the design of the instrument to increase its versatility and optimize its general performance. These features are described and discussed below. Other detailed comments will be found in the service manual.

Bake-out Heaters. - To insure rapid clean up of the instrument after exposure to contaminant gases (particularly water vapor), two external heating elements have been provided for the cold cathode ion source and also for the quadrupole analyzer. In addition, a special pumping port has been installed on the analyzer and multiplier sections. This port provides a relatively high conductance auxiliary egress for internal outgassing.

The bake-out heaters are wired on separate circuits so that either the ion source or analyzer housing or both may be heated. The analyzer is provided with an aluminum heat shield to minimize heat radiated to the electronics components inside the box. Sensors are provided to monitor the bake-out temperature. Control of these temperatures must be provided by external circuitry. Detailed electrical specifications for the heating elements and for the temperature sensors are given in the operating manual.

Ion-Source Entrance Ports. - Two entrance ports are provided on the ion source. These ports are positioned transversely to the axis of the analyzer and are diametrically opposite one another. Standard miniature flanges are provided to cover one of the ports if uni-directional response is desired. These ports could be fitted with remotely operated baffle covers to alternately measure gas fluxes from two opposite directions.

Multiplier Gain Measurements. - The output end of the electron multiplier is provided with separate connectors for the first dynode and high voltage terminal of the electron multiplier. In normal operation these terminals are jumpered with a short coaxial cable to apply high voltage to the dynodes. By removing the jumper cable, a direct measurement of the ion current arriving at the first dynode can be made. In conjunction with the normal connections, a relative multiplier gain measurement may be made to check the sensitivity of the spectrometer on a periodic basis. The multiplier high voltage power supply is adjustable should gain adjustment be required. Reference should be made to the operating manual for gain adjustment.

Total Cathode Current (Ion Source). - The ion source has two electrical connections; one for the anode and one for the cathodes. Should a measurement of total ion source pressure be desirable, an auxiliary electrometer (not supplied) can be connected to the cathode terminal. Such a measurement can be helpful in an end-to-end check of spectrometer sensitivity.

#### CONCLUSIONS

The overall performance of the laboratory prototype RGA has generally come very close to the original design goals and guidelines. One exception appears to be the average power consumption which is about 50% larger than the original design goal value which was probably overly restrictive. The resolving power, dynamic range, and fast scan time have also approximated the original guidelines. The sensitivity of the basic instrument is high, which should permit a reduction in the lower limit of partial pressure detectability if a future need arises.